Sarcospan-dependent Akt activation is required for utrophin expression and muscle regeneration

Jamie L. Marshall,[1] Johan Holmberg,[1] Eric Chou,[1] Amber C. Ocampo,[1] Jennifer Oh,[1] Joy Lee,[1] Angela K. Peter,[1] Paul T. Martin,[3,4] and Rachelle H. Crosbie-Watson[1,2]

[1]Department of Integrative Biology and Physiology and [2]Molecular Biology Institute, University of California, Los Angeles, Los Angeles, CA 90095
[3]Center for Gene Therapy, The Research Institute, Nationwide Children's Hospital, and [4]Department of Pediatrics, Ohio State University College of Medicine and College of Public Health, Columbus, OH 43205

Utrophin is normally confined to the neuromuscular junction (NMJ) in adult muscle and partially compensates for the loss of dystrophin in *mdx* mice. We show that Akt signaling and utrophin levels were diminished in sarcospan (SSPN)-deficient muscle. By creating several transgenic and knockout mice, we demonstrate that SSPN regulates Akt signaling to control utrophin expression. SSPN determined α-dystroglycan (α-DG) glycosylation by affecting levels of the NMJ-specific glycosyltransferase Galgt2. After cardiotoxin (CTX) injury, regenerating myofibers express utrophin and Galgt2-modified α-DG around the sarcolemma. SSPN-null mice displayed delayed differentiation after CTX injury caused by loss of utrophin and Akt signaling. Treatment of SSPN-null mice with viral Akt increased utrophin and restored muscle repair after injury, revealing an important role for the SSPN-Akt-utrophin signaling axis in regeneration. SSPN improved cell surface expression of utrophin by increasing transportation of utrophin and DG from endoplasmic reticulum/Golgi membranes. Our experiments reveal functions of utrophin in regeneration and new pathways that regulate utrophin expression at the cell surface.

Introduction

Duchenne muscular dystrophy (DMD) is an X-linked disorder that affects ∼1/3,500 live male births and is characterized by progressive skeletal muscle deterioration. DMD results from mutations in the *dystrophin* gene (Hoffman et al., 1987), which leads to loss of dystrophin protein and renders the sarcolemma susceptible to contraction-induced damage (Campbell and Kahl, 1989; Yoshida and Ozawa, 1990; Petrof et al., 1993). Dystrophin is a component of the dystrophin–glycoprotein complex (DGC), which is composed of integral and peripheral membrane proteins that physically connect the ECM to the intracellular cytoskeleton (Campbell and Kahl, 1989; Ervasti et al., 1990, 1991; Yoshida and Ozawa, 1990; Ervasti and Campbell, 1991). Recently, developments in force measurements have demonstrated that the DGC contributes to lateral force during muscle contractility (Ramaswamy et al., 2011). The most common in vivo model for DMD is the *mdx* mouse, which has an inherited, X-linked recessive mutation in dystrophin, resulting in loss of dystrophin protein from the sarcolemma (Allamand and Campbell, 2000). The *mdx* muscle is characterized by an absence of the entire DGC complex from the sarcolemma, which disrupts interaction of the sarcolemma with its surrounding ECM (Ervasti and Campbell, 1993). The significant reduction in muscle cell adhesion leads to cycles of muscle fiber degeneration/regeneration and eventually muscle cell death. Loss of appropriate connections between the muscle cell membrane and the ECM has emerged as a critical initiating event in many forms of muscular dystrophy and muscle-wasting disorders.

Within the DGC, dystrophin is anchored to the intracellular face of the sarcolemma by attachment to dystroglycan (DG).

Correspondence to Rachelle H. Crosbie-Watson: rcrosbie@physci.ucla.edu

A.K. Peter's present address is Dept. of Medicine, University of California, San Diego, La Jolla, CA 92093.

Abbreviations used in this paper: CT, cytotoxic T cell; CTX, cardiotoxin; DG, dystroglycan; DGC, dystrophin–glycoprotein complex; DMD, Duchenne muscular dystrophy; eMHC, embryonic myosin heavy chain; GalNAc, *N*-acetyl galactosamine; GAPDH, glyceraldehyde 3-phosphate dehydrogenase; GlcNAc, *N*-acetyl glucosamine; H&E, hematoxylin and eosin; IGF-R, insulin-like growth factor receptor; IP, immunoprecipitation; MCK, muscle creatine kinase; *myd*, *myodystrophy*; NMJ, neuromuscular junction; RIPA, radioimmunoprecipitation assay; rtTA, reverse tetracycline transactivator; SG, sarcoglycan; SSPN, sarcospan; sWGA, succinylated WGA; Tg, transgene; UGC, utrophin–glycoprotein complex; WFA, *Wisteria floribunda* agglutinin; WT, wild type.

The Rockefeller University Press $30.00
J. Cell Biol. Vol. 197 No. 7 1009–1027
www.jcb.org/cgi/doi/10.1083/jcb.201110032

DG is a core component of the DGC and consists of two subunits produced from a single mRNA that is posttranslationally processed into α- and β-DG (Ibraghimov-Beskrovnaya et al., 1992, 1993). The N terminus of dystrophin interacts with the intracellular F-actin cytoskeleton, and the C-terminal region of dystrophin interacts with β-DG (Ervasti, 2007). Recent data have revealed that plectin-1, which binds F-actin and β-DG, contributes to the stability of these interactions (Rezniczek et al., 2007). Sarcospan (SSPN) forms a tight subcomplex with four sarcoglycans (SGs; α-, β-, γ-, and δ-SG), which are single-pass integral membrane glycoproteins (Crosbie et al., 1999a; Miller et al., 2007). The SG–SSPN subcomplex anchors α-DG to the sarcolemma, and absence of this subcomplex in SG-deficient muscle leads to destabilization of α-DG from the cell surface (Crosbie et al., 1997b, 1999b, 2000; Holt et al., 1998).

Identification of mechanisms that restore cell surface–ECM connection has the potential to affect a broad range of muscle-wasting disorders. Introduction of α7β1 integrin or the utrophin–glycoprotein complex (UGC) into *mdx* muscle functionally replaces the DGC by improving muscle cell adhesion to the ECM, thereby stabilizing the sarcolemma during contraction (Deconinck et al., 1997b; Gilbert et al., 1999; Burkin et al., 2001; Squire et al., 2002; Deol et al., 2007; Liu et al., 2012). Interestingly, these adhesion complexes are normally enriched at the myotendinous junction and postsynaptic region of the neuromuscular junction (NMJ; Khurana et al., 1991; Nguyen et al., 1991; Matsumura et al., 1992; Zhao et al., 1992; Martin et al., 1996; Tinsley et al., 1996; Grady et al., 1997a,b, 2000; Tinsley et al., 1998a; Burkin and Kaufman, 1999). Elegant studies have demonstrated that overexpression of α7β1D integrin or utrophin in dystrophin-deficient *mdx* mice results in amelioration of pathology (Tinsley et al., 1996, 1998b; Deconinck et al., 1997a; Rafael et al., 1998; Gilbert et al., 1999; Burkin et al., 2001, 2005; Fisher et al., 2001; Squire et al., 2002; Deol et al., 2007; Odom et al., 2008; Sonnemann et al., 2009; Liu et al., 2012). Utrophin is an autosomal homologue of dystrophin and interacts with the DGs and the SG–SSPN subcomplex to form the UGC, in which utrophin replaces the function of dystrophin (Love et al., 1989; Khurana et al., 1991; Matsumura et al., 1992; Peter et al., 2008).

We and others have previously reported that expression of activated Akt transgenes (Tgs) in *mdx* skeletal muscle causes broad sarcolemma localization of utrophin, providing evidence that activation of Akt signaling pathways is an important mechanism regulating utrophin expression (Peter and Crosbie, 2006; Blaauw et al., 2008, 2009; Peter et al., 2009; Kim et al., 2011). Introduction of the cytotoxic T cell (CT) *N*-acetyl galactosamine (GalNAc) transferase (*Galgt2*), the enzyme that adds a terminal β1,4 GalNAc glycan to create the CT antigen, ameliorates the dystrophic pathology in *mdx* mice by increasing the CT antigen modification of α-DG and broadening the UGC expression to the extrasynaptic sarcolemma (Nguyen et al., 2002; Xu et al., 2007a). We previously demonstrated that introducing SSPN into *mdx* mice alleviated symptoms of muscular dystrophy by increasing levels of utrophin around the extrasynaptic sarcolemma (Peter et al., 2008). SSPN is a 25-kD tetraspanin-like protein that possesses four transmembrane domains and two extracellular loops with binding domains for DG and the SGs (Crosbie et al., 1997a; Miller et al., 2007). In the current study, we investigate these mechanisms by testing whether SSPN activates pathways that are known to regulate utrophin in skeletal muscle.

Results

SSPN increases levels of all major adhesion complexes in a dose-dependent fashion

We generated new lines of SSPN transgenic mice exhibiting 0.5-, 1.5-, and 3.0-fold levels of SSPN overexpression with the rationale that analyzing such model systems would reveal SSPN-dependent molecular events that lead to increased utrophin expression and amelioration of pathology. SSPN-Tg males (wild type$^{0.5}$ [WT$^{0.5}$], WT$^{1.5}$, and WT$^{3.0}$) were crossed with *mdx* heterozygous females to generate dystrophin-deficient mice carrying the SSPN-Tg (*mdx*$^{0.5}$, *mdx*$^{1.5}$, and *mdx*$^{3.0}$). Exogenous SSPN was robustly detected at the sarcolemma in all lines of transgenic WT mice, whereas higher levels of SSPN-Tg were required for stable membrane expression in *mdx* mice (Fig. 1 A). Interestingly, we found that 1.5- and 3.0-fold overexpression of SSPN in WT and *mdx* muscle increased localization of utrophin, dystrophin, and β1D integrin around the sarcolemma, demonstrating that SSPN positively affects protein levels of the major adhesion complexes in muscle (Fig. 1, B–D). Expression of the DGs and SGs was restored around the extrasynaptic sarcolemma of 1.5-fold SSPN transgenic *mdx* mice (*mdx*$^{1.5}$) similar to the 3.0-fold SSPN transgenic *mdx* mice (*mdx*$^{3.0}$), demonstrating that even lower levels of SSPN overexpression (1.5- vs. 3.0-fold) are able to stabilize the UGC and DGC around the extrasynaptic sarcolemma in WT and *mdx* mice (Fig. S1, A and B). Densitometry of immunoblots (Fig. S1 B) reveals that SSPN increases utrophin expression in a stepwise fashion (Fig. 1 E) without affecting utrophin mRNA levels (Fig. 1 F).

To investigate the histopathological consequences of SSPN expression in dystrophin-deficient muscle, transverse cryosections of transgenic WT (WT$^{0.5}$, WT$^{1.5}$, and WT$^{3.0}$) and *mdx* (*mdx*$^{0.5}$, *mdx*$^{1.5}$, and *mdx*$^{3.0}$) quadriceps were stained with hematoxylin and eosin (H&E; Fig. 2 A). Central nucleation, a marker of myofiber regeneration, was quantified from H&E-stained quadriceps samples. *mdx* muscles displayed elevated levels (50%) of regenerated myofibers with central nuclei, which was not altered in *mdx*$^{0.5}$ and *mdx*$^{1.5}$ mice (Fig. 2 B). However, amelioration of dystrophic pathology was evident in *mdx*$^{3.0}$ muscle, as indicated by decreased central nucleation (Peter et al., 2008). As an additional test of *mdx* pathology, we performed a standard Evans blue dye tracer assay to assess membrane damage in SSPN transgenic *mdx* mice (Straub et al., 1997). Sarcolemmal integrity was not improved in *mdx*$^{0.5}$ and *mdx*$^{1.5}$ muscle (unpublished data), whereas *mdx*$^{3.0}$ muscle exhibited dramatic reductions in membrane damage (Peter et al., 2008).

SSPN determines glycosylation of α-DG

Increasing cell surface glycosylation of α-DG by genetic introduction of glycosyltransferases improves utrophin levels at the extrasynaptic sarcolemma (Nguyen et al., 2002; Xu et al., 2007a). NMJ-specific glycosylation of α-DG is catalyzed by

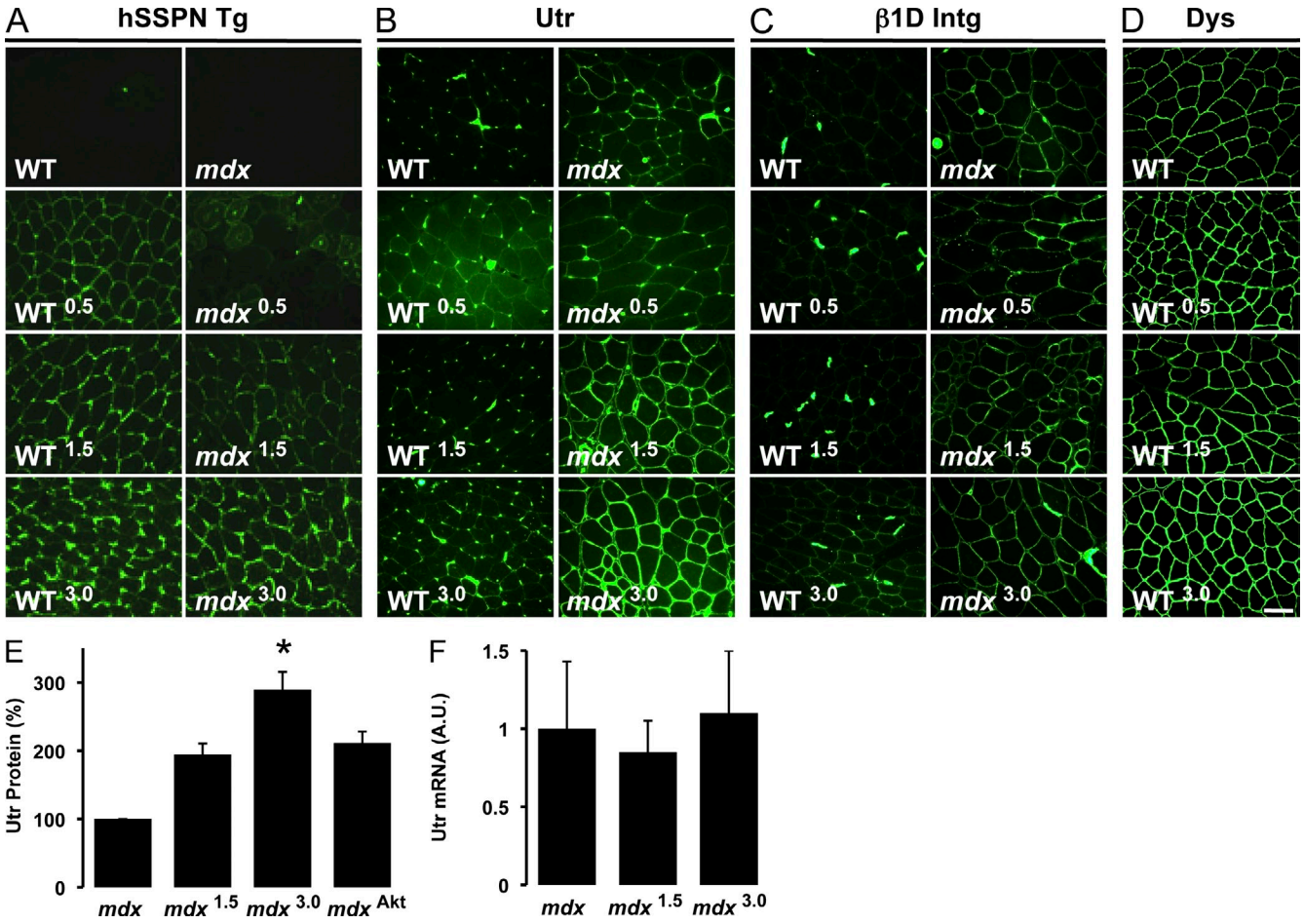

Figure 1. **SSPN increases expression of utrophin, dystrophin, and integrin.** (A–D) Transverse cryosections of quadriceps muscles were stained with indicated antibodies. Bar, 50 µm. (E) Levels of utrophin were quantified by densitometry of protein bands from immunoblotting of quadriceps protein samples. Values are expressed relative to *mdx* levels (100%). Error bars represent standard deviation of the mean (n = 3 mice per genotype). Statistical significance of the difference between samples was determined by Student's t test (*, $P < 0.05$). (F) Quantitative RT-PCR was used to investigate whether overexpression of SSPN altered RNA levels of utrophin (Utr). RNA was isolated from *mdx*, $mdx^{1.5}$, and $mdx^{3.0}$ skeletal muscle. mRNA expression levels were normalized to GAPDH. Data are expressed relative to that of *mdx* controls. Error bars represent standard deviation. Utrophin mRNA levels in Akt transgenic *mdx* mice were identical to *mdx* (Peter et al., 2009). A.U., arbitrary unit; Intg, integrin; Dys, dystrophin; hSSPN, human SSPN.

the Galgt2 that, like utrophin, is confined to the NMJ in normal skeletal muscle (Xia et al., 2002). Galgt2 catalyzes addition of the terminal β1,4 GalNAc residue onto the CT carbohydrate antigen (Smith and Lowe, 1994). Overexpression of Galgt2 in *mdx* muscle increases CT antigen modification of α-DG that enhances laminin-binding activity of α-DG (Nguyen et al., 2002; Xia et al., 2002).

To investigate whether SSPN affects glycosylation in a similar manner, we used the lectin *Wisteria floribunda* agglutinin (WFA) as a marker for NMJ-specific glycosylation of α-DG. WFA preferentially binds carbohydrate structures terminating in GalNAc linked to the 3 or 6 position of galactose. Because β1,4 GalNAc is an essential glycan of the CT carbohydrate, WFA binds glycoproteins bearing the CT antigen (Martin and Sanes, 1995; Hoyte et al., 2002; Xia et al., 2002; Martin, 2003; Xu et al., 2007a). We show that WFA binding is localized to NMJs (Fig. S2 A) in normal muscle, which are sites of enrichment for dystrophin- and utrophin-containing complexes in normal muscle. WFA binding is increased around the extrasynaptic sarcolemma of *mdx* muscle cryosections (Figs. 3 A and S2 B) in a pattern identical to that of *mdx* muscle transfected with the Galgt2 plasmid (Durko et al., 2010). We found that WFA binding to $mdx^{0.5}$, $mdx^{1.5}$, and $mdx^{3.0}$ muscle was significantly improved around the extrasynaptic sarcolemma (Fig. 3 A) in a dose–response that is similar to utrophin expression (Fig. 1 B). To investigate the dependency of WFA binding on utrophin expression, we demonstrate that WFA binding is absent in utrophin-deficient *mdx* mice (Fig. 3 A). However, overexpression of constitutively active Akt in *mdx* muscle did not alter WFA binding (Fig. 3 B) despite increases in utrophin (Blaauw et al., 2008, 2009; Peter et al., 2009; Kim et al., 2011), revealing that Akt alone is unable to drive cell surface glycosylation in dystrophin deficiency.

The observation that SSPN improves cell surface glycosylation and utrophin expression suggests that SSPN affects glycan modifications of one or more utrophin-associated glycoproteins. To identify these proteins, we subjected skeletal muscle homogenates from SSPN-Tg and SSPN-Tg:*mdx* mice to WFA lectin affinity chromatography. Enriched proteins were eluted from solid-phase WFA columns using GalNAc and analyzed by

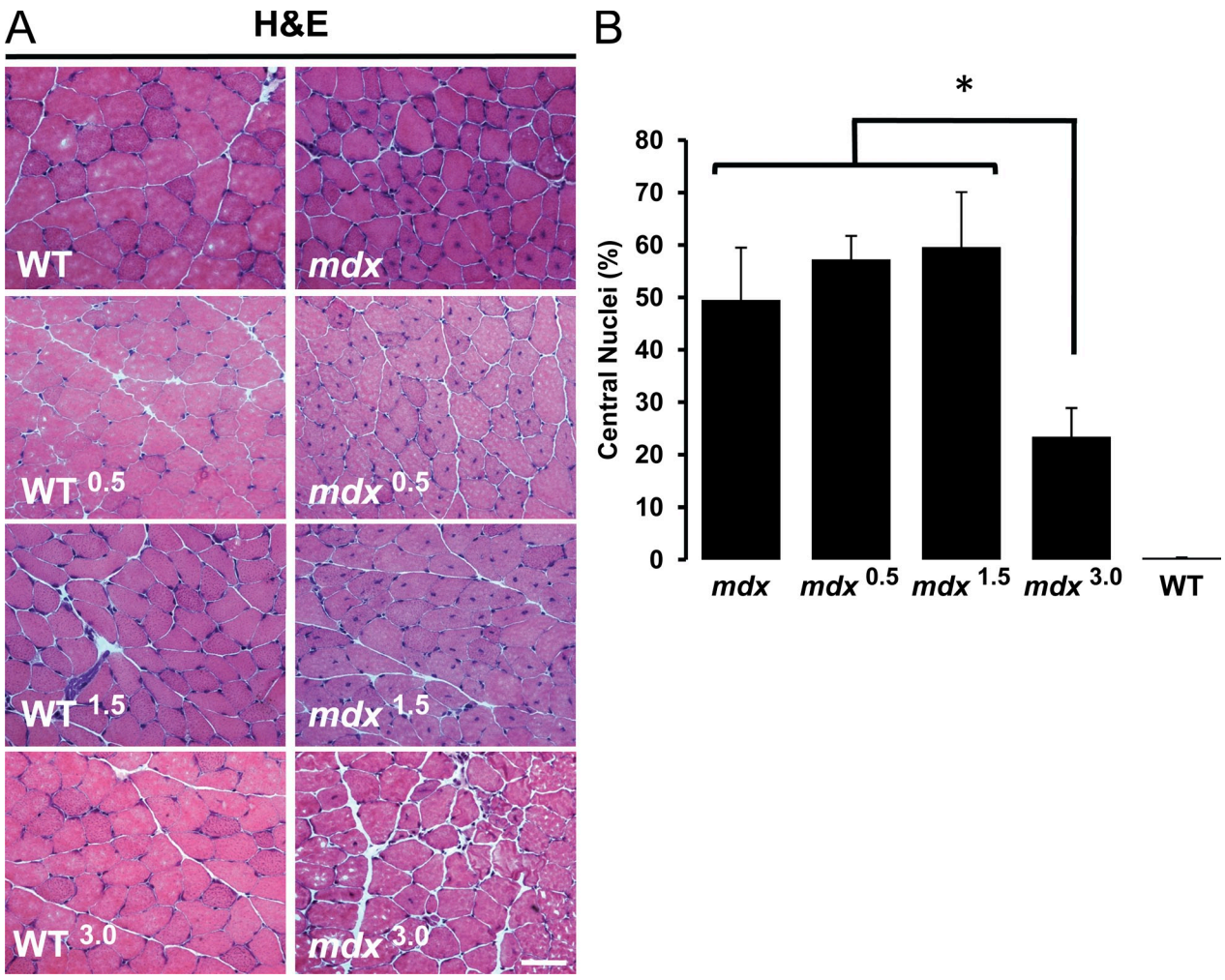

Figure 2. **Threefold SSPN levels are required for *mdx* rescue effect.** (A) Transverse cryosections of quadriceps muscle from non-Tg and SSPN-Tg mice were stained with H&E to visualize muscle pathology. Bar, 50 µm. (B) Muscle regeneration was evaluated by quantification of myofibers with central nuclei. Central nucleation values for SSPN-Tg muscles were identical to WT controls (not depicted). Data for threefold SSPN-Tg:*mdx* ($mdx^{3.0}$) samples is taken from Peter et al. (2008) and shown for comparison. Error bars represent standard deviation of the mean (n = 6 quadriceps per genotype). Statistical significance of the difference between indicated samples was determined by Student's t test (*, $P < 0.05$).

ligand overlay assays and immunoblotting. To identify proteins that bound directly to WFA, nitrocellulose transfers of protein eluates were overlayed with biotinylated WFA. Robust WFA binding was evident in *mdx* muscle, which was further increased in $mdx^{1.5}$ and $mdx^{3.0}$ samples (Fig. 3, C and D). For all samples analyzed, WFA bound to a glycoprotein with a molecular mass identical to that of α-DG. This same WFA-reactive protein also bore the CT2 antigen as revealed by immunoblotting with CT2-specific antibodies (Fig. 3 C). We also show that the CT2 antigen antibody staining was highest in SSPN transgenic *mdx* samples. Identification of α-DG as the WFA and CT antigen-reactive glycoprotein was confirmed by immunoblotting with antibodies to α-DG (Fig. 3, C and D). Overexpression of Akt in *mdx* muscle did not improve WFA binding to α-DG in ligand overlay assays (Fig. 3 E), supporting immunofluorescence data (Fig. 3 B). Densitometry of WFA binding as a function of DG protein levels was performed to evaluate the relative extent of glycosylation on α-DG. We found that α-DGs from $mdx^{1.5}$ and $mdx^{3.0}$ were decorated with 1.8-fold more WFA-reactive glycans relative to *mdx* controls (Fig. 3 F).

Previous work has demonstrated that α-DG is the predominant glycoprotein modified with the CT carbohydrate in both *mdx* and Galgt2 transgenic skeletal muscle (Nguyen et al., 2002). Increased Galgt2 activity in *mdx* mice is the result of a twofold elevation in *Galgt2* mRNA levels in *mdx* muscle relative to WT controls (Nguyen et al., 2002). Results from quantitative RT-PCR reveal that SSPN does not affect *Galgt2* transcript levels in either normal or dystrophin-deficient muscles (Fig. 3 G). To investigate *Galgt2* at the protein level, we probed immunoblots of total muscle protein lysates with antibodies to Galgt2 and found that all samples exhibited similar Galgt2 antibody staining per milligram of muscle protein (Fig. 3 H). Our data demonstrate that overexpression of SSPN alters glycosylation of α-DG without affecting the mRNA transcript or protein levels of Galgt2.

SSPN improves α-DG binding to laminin in dystrophin deficiency

SSPN transgenic expression improved laminin expression at the sarcolemma in both WT and dystrophin-deficient muscle

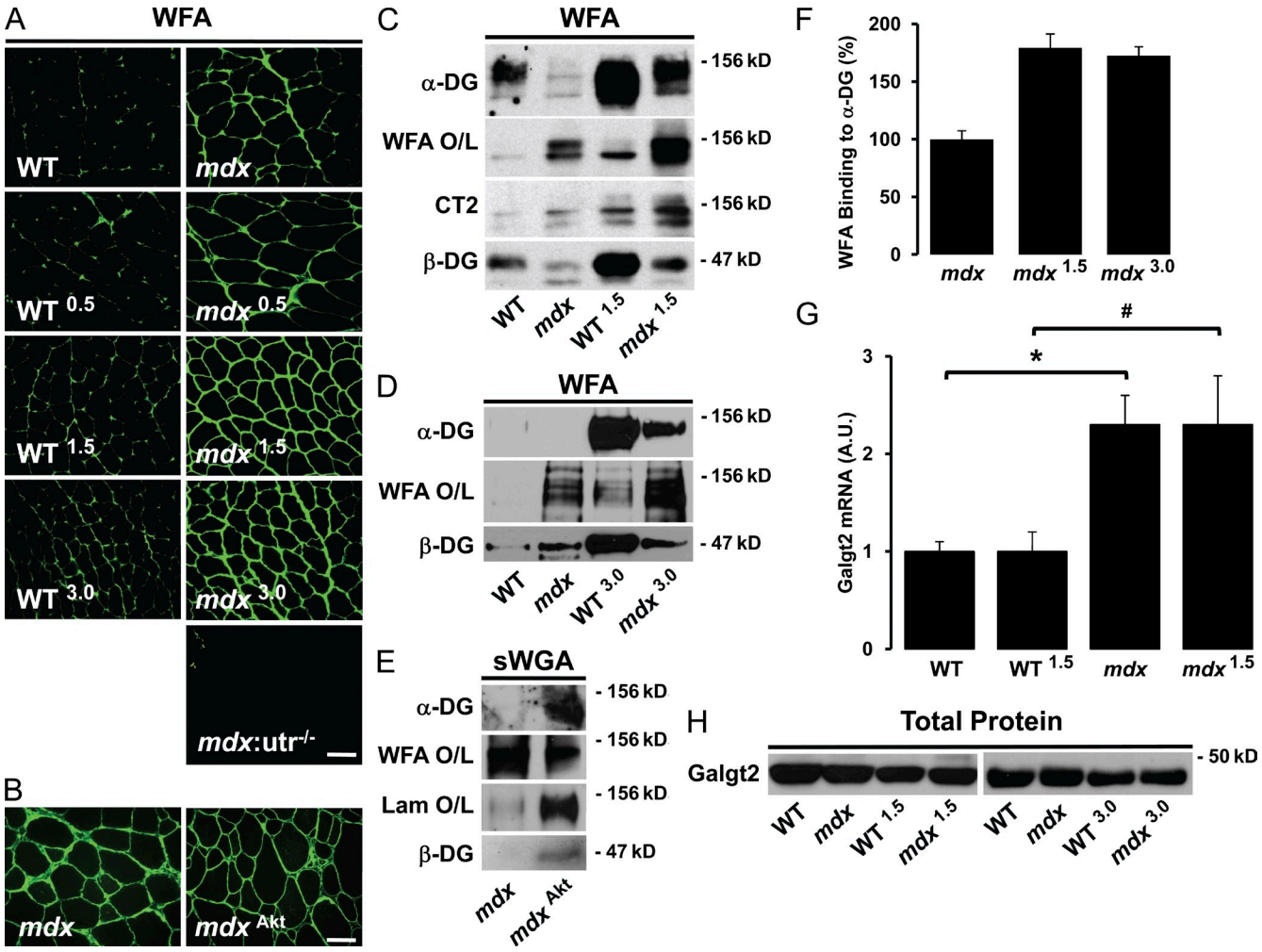

Figure 3. **SSPN increases cell surface glycosylation in *mdx* muscle.** (A and B) Transverse cryosections of quadriceps muscles from SSPN-Tg (A) or Akt transgenic (B) muscles were stained with biotinylated *Wisteria floribunda* agglutinin (WFA) and visualized by indirect immunofluorescence. Bars, 50 µm. (C) Skeletal muscle protein lysates from the indicated mouse models were enriched by WFA lectin affinity chromatography (WFA enrichment) and analyzed with indicated antibodies and overlayed (O/L) with WFA lectin (WFA O/L). (D) Skeletal muscle protein lysates were enriched by WFA lectin affinity chromatography (WFA enrichment) and subjected to the same analysis as described in C. (E) WFA and laminin overlay assays were performed on protein lysates enriched with succinylated WGA (sWGA) lectin chromatography from *mdx* and Akt transgenic *mdx* (*mdx*^{Akt}) muscle. Mice were treated with doxycycline to induce Akt expression in skeletal muscle as described previously (Peter et al., 2009). Laminin overlays (Lam O/L) represent binding to immobilized α-DG on nitrocellulose transfers. Immunoblotting with antibodies to α-DG is shown. (F) Levels of WFA binding to α-DG were quantitated by densitometry of bands from overlay assays, and data are expressed relative to *mdx* levels (100%). Error bars represent standard deviation of the mean (n = 2–3 muscle preps per genotype). (G) Quantitative RT-PCR was used to investigate whether overexpression of SSPN alters RNA levels of CT GalNAc transferase (*Galgt2*). RNA was isolated from WT, WT$^{1.5}$, *mdx*, and *mdx*$^{1.5}$ skeletal muscle. Data are expressed relative to non-Tg WT controls. Error bars represent standard error of the mean (*, $P < 0.05$; #, $P < 0.01$; n = 3). The increase in endogenous *Galgt2* gene expression in *mdx* mice relative to WT non-Tg supports previous observations (Xu et al., 2007a,b). (H) Skeletal muscle from indicated mouse models was solubilized in modified RIPA buffer, and 50-µg protein samples were resolved by SDS-PAGE. Immunoblotting was performed with antibodies against Galgt2. A.U., arbitrary unit; utr, utrophin.

(Fig. 4 A), which is supported by immunoblots of skeletal muscle homogenates probed with laminin antibodies (Fig. 4 B). We found that SSPN overexpression did not significantly alter levels of agrin in 1.5-fold SSPN-Tg:*mdx* mice, but plectin-1 was dramatically increased in *mdx*$^{1.5}$ muscle (Fig. 4 B). Plectin-1 binds to intracellular cytoskeletal proteins, including F-actin, vimentin, and desmin as well as to β-DG, dystrophin, and utrophin (García-Alvarez et al., 2003; Hijikata et al., 2003; Litjens et al., 2005; Rezniczek et al., 2007). This further suggests that overexpression of SSPN facilitates and/or strengthens the association of the UGC, leading to its extrasynaptic stabilization in dystrophin-deficient mice. Laminin binding to α-DG was assessed by overlaying laminin protein onto skeletal muscle lysates enriched by succinylated WGA (sWGA) lectin chromatography, which binds glycoproteins bearing GlcNAc glycans, including the DGC and UGC (Crosbie et al., 1997b). Laminin binding to α-DG was restored to normal levels in the *mdx*$^{3.0}$ and not in *mdx*$^{1.5}$ samples (Fig. 4, C and D), revealing that restoration of laminin binding is necessary for amelioration of *mdx* pathology.

SSPN facilitates transportation of utrophin-DG from ER/Golgi to the cell surface

Based on the observation that many tetraspanins facilitate membrane trafficking of cell surface receptors, such as EGF receptor

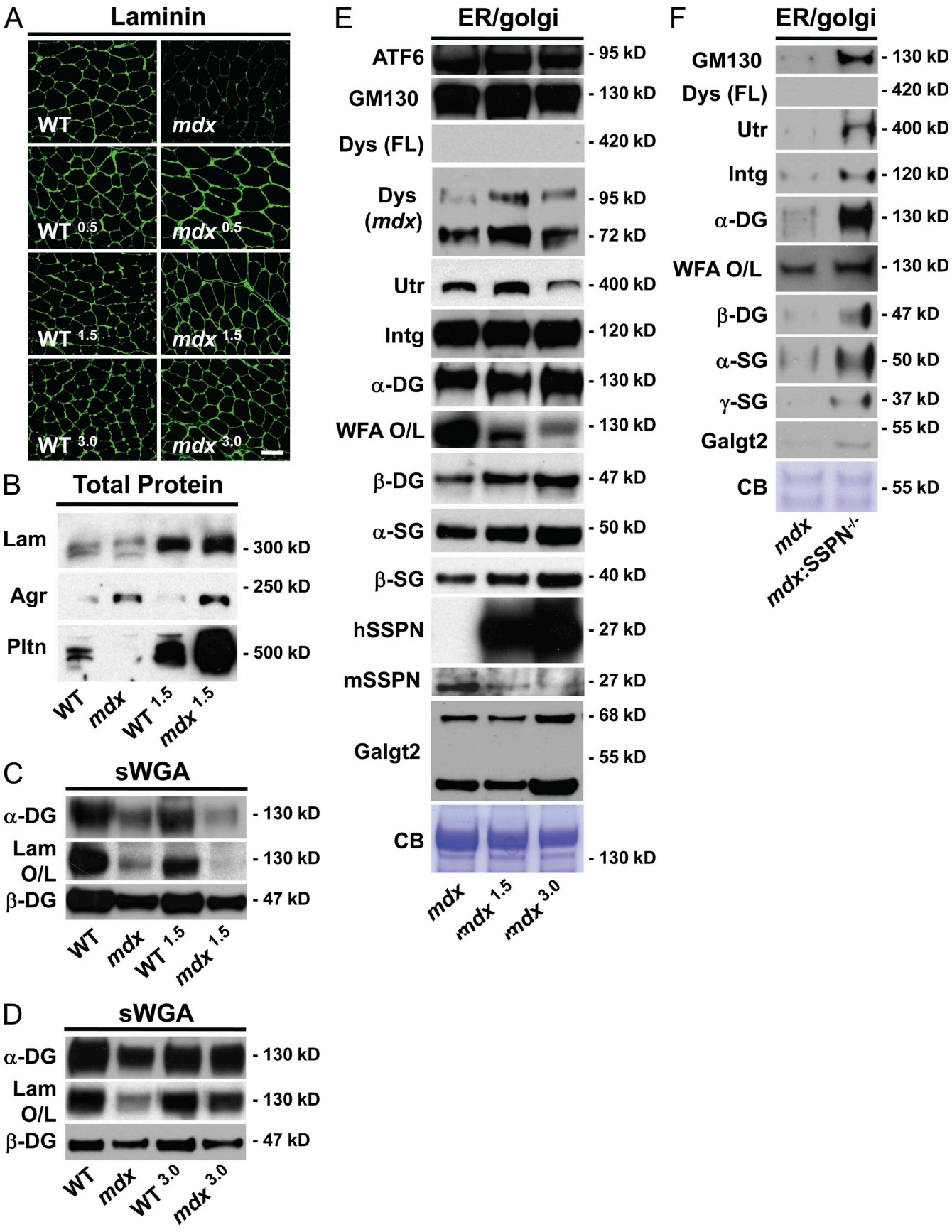

Figure 4. **SSPN facilitates transportation of the UGC to the sarcolemma to restore laminin binding.** (A) Transverse cryosections of quadriceps muscles from the indicated mice were stained with antilaminin antibodies. Bar, 50 µm. (B) Skeletal muscles were solubilized in RIPA buffer, and 50 µg of each protein lysate was resolved by SDS-PAGE. Immunoblotting was performed with indicated antibodies. GAPDH and Coomassie blue (CB) loading controls

and integrins (Liu et al., 2007), we hypothesized that SSPN increases laminin binding by enhancing transportation of laminin-binding receptors to the cell surface. To explore this possibility, we purified ER/Golgi membrane vesicles from *mdx* and SSPN transgenic *mdx* skeletal muscle using standard protocols. Proteins from purified vesicles were analyzed by WFA overlay assay in addition to immunoblotting with antibodies to each of the UGC components as well as integrin. We found that the ER/Golgi compartments from *mdx* muscle contained robust levels of utrophin and its associated proteins (Fig. 4 E), whereas these same proteins are barely detectable at the *mdx* sarcolemma (Figs. 1 and S1). We also demonstrate, for the first time, that the ER/Golgi exhibits an abundance of truncated N-terminal dystrophin fragments produced from the premature termination codon (*mdx* mutation) in the dystrophin gene (Fig. 4 E). These dystrophin fragments lack the C-terminal region that forms the β-DG–interacting domain. We interpret these data to mean that truncated dystrophin fragments as well as utrophin are synthesized in *mdx* muscle but then retained in intracellular membrane compartments rather than properly transported to the sarcolemma. DGC and UGC proteins were detected at low levels in ER/Golgi membranes isolated from WT muscle (unpublished data).

Interestingly, utrophin levels are significantly reduced in ER/Golgi preparations from $mdx^{1.5}$ and $mdx^{3.0}$ samples (Fig. 4 E). WFA overlays of nitrocellulose transfers reveal significant GalNAc glycan modification of α-DG in ER/Golgi isolations from *mdx* muscle (Fig. 4 E). In contrast to the cell surface (Fig. 3 A), WFA binding to α-DG was significantly reduced in ER/Golgi vesicles from $mdx^{1.5}$ and $mdx^{3.0}$ (Fig. 4 E). Supporting the increase in WFA binding to α-DG at the sarcolemma in SSPN transgenic *mdx* mice, overexpression of SSPN increases the amount of Galgt2 protein that is available to glycosylate α-DG in the ER/Golgi (Fig. 4 E). The loss of SSPN from *mdx* muscle results in an increase in utrophin and GalNAc glycan-modified α-DG in the ER/Golgi compared with *mdx* muscle (Fig. 4 F). SSPN specifically affects the transportation of utrophin and its associated α-DG, accounting for the depletion of such complexes from the ER/Golgi. SSPN did not appear to affect levels of mutant dystrophin, the SGs, or β1D integrin found in the ER/Golgi, suggesting that SSPN's effect is specific for the NMJ-specific utrophin–DG complexes.

Utrophin and glycosylation of α-DG are diminished in SSPN-null mice

We found that SSPN-deficient muscle exhibited normal localization of utrophin and enrichment of WFA binding to NMJ structures (Fig. S3, A and B). Although SSPN-deficient mice have been reported to maintain normal muscle physiology without perturbation of the DGC complex (Lebakken et al., 2000), we found that SSPN-deficient mice exhibit defects in the UGC. In fact, the SGs and integrin are reduced from the sarcolemma in SSPN-deficient muscle (Fig. S3 C). Analysis of sWGA-enriched samples revealed that levels of utrophin and α/β-DG are significantly reduced upon loss of SSPN (Fig. 5 A). Furthermore, analysis of WFA enrichments of skeletal muscle protein lysates revealed decreased glycosylation of α-DG in SSPN-deficient muscle, demonstrating that SSPN is an important regulator of posttranslational modification of α-DG (Fig. 5 B). To biochemically determine whether loss of SSPN affects the UGC, we isolated this complex from skeletal muscle of SSPN-null mice using sWGA lectin affinity chromatography followed by ultracentrifugation on 5–20% sucrose gradients. Only proteins that are tightly associated are maintained as a complex and migrate together during ultracentrifugation. Fractions were collected and analyzed by immunoblotting and WFA lectin overlay assay. Loss of SSPN reduced GalNAc modification of α-DG (denoted by WFA binding) and dramatically diminished utrophin association with the DG (Fig. 5 C). We noted a trend of decreased Galgt2 mRNA and protein levels in SSPN-null muscle compared with WT controls (Fig. 5, D and E), which accounts for the decreased glycosylation of α-DG revealed by low WFA binding to α-DG in SSPN deficiency. Utrophin mRNA levels are not altered by loss of SSPN (Fig. 5 E), providing further support that SSPN regulates utrophin protein in a posttranslational manner.

SSPN regulates utrophin levels and glycosylation of α-DG in mouse models of dystroglycanopathy

A group of muscular dystrophies referred to as the dystroglycanopathies results from hypoglycosylation of α-DG, which impairs DG function and muscle cell adhesion. A spontaneous mutation in the *LARGE* gene, which encodes a putative GlcNAc glycosyltransferase, causes muscular dystrophy in the *myodystrophy* (*myd*) mouse (Grewal et al., 2001). In *myd* muscle, α-DG is hypoglycosylated and exhibits severely reduced ligand binding activity as a result of loss of the glycan-laminin binding domain on α-DG (Holzfeind et al., 2002; Michele et al., 2002). LARGE mediates *O*-mannosyl phosphorylation of the mucin domain on α-DG by direct interaction with α-DG (Kanagawa et al., 2004; Yoshida-Moriguchi et al., 2010). Because SSPN regulates glycan modification of α-DG in WT and *mdx* mice, we set out to determine whether SSPN would evoke similar effects in a mouse model of dystroglycanopathy.

For these experiments, we first tested whether deficiency of the LARGE glycosyltransferase affected NMJ glycosylation of α-DG. We found that loss of the LARGE enzyme increases utrophin and SSPN staining and WFA binding around the extrasynaptic sarcolemma of *myd* muscle, as indicated by lectin overlay of skeletal muscle cryosections (Fig. 6 A). Introduction

are shown in Fig. S1. (C and D) sWGA-enriched protein samples were analyzed for laminin binding. Laminin overlays (Lam O/L) represent binding to immobilized α-DG on nitrocellulose transfers. Blots were also stained with antibodies to α- and β-DG as indicated. (E) Proteins in ER and Golgi membranes (ER/Golgi) were purified from *mdx*, $mdx^{1.5}$, and $mdx^{3.0}$ muscles. Protein samples were resolved by SDS-PAGE and subjected to immunoblotting with the indicated antibodies. Staining with endogenous (mouse SSPN [mSSPN]) and exogenous (human SSPN [hSSPN]) is shown. ATF6 and GM130 served as protein markers for the ER and Golgi, respectively. (F) Proteins in ER and Golgi membranes (ER/Golgi) were purified from *mdx* (*mdx*) and SSPN-deficient *mdx* (*mdx*:$SSPN^{-/-}$) muscles and analyzed by immunoblotting. WFA binding to α-DG was assessed using WFA ligand overlay assays (WFA O/L). Lam, laminin; O/L, overlay; Agr, agrin; Pltn, plectin-1; Dys, dystrophin; FL, full length; Utr, utrophin; Intg, integrin.

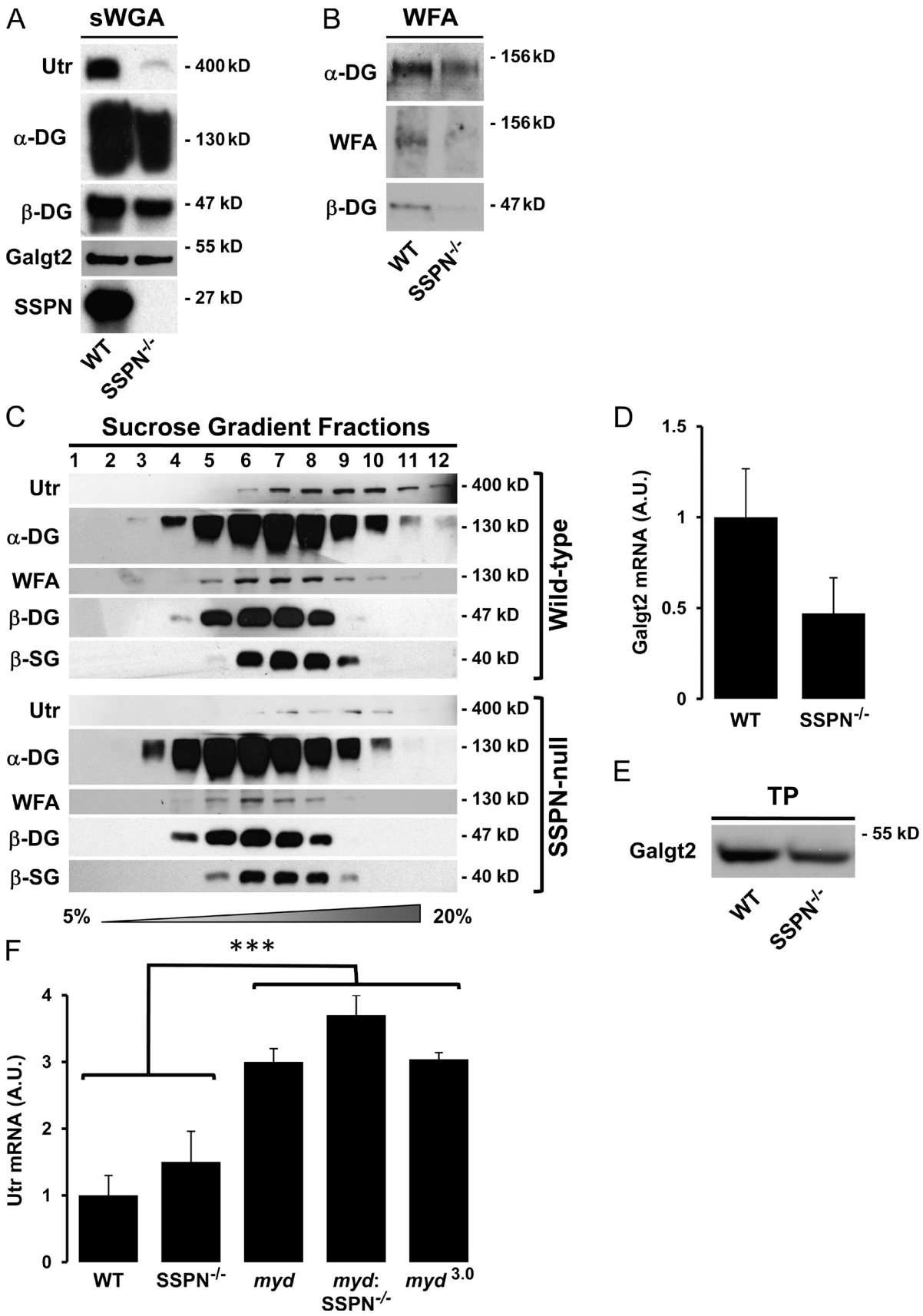

Figure 5. **Loss of SSPN impairs utrophin expression and glycosylation of α-DG.** (A) Skeletal muscle lysates from wild-type (WT) and SSPN-deficient ($SSPN^{-/-}$) mice were enriched by sWGA lectin chromatography, and 10-µg protein samples were immunoblotted with the indicated antibodies. (B) Skeletal muscle protein lysates from WT muscle and SSPN-null ($SSPN^{-/-}$) mice were enriched by WFA lectin affinity chromatography, and nitrocellulose transfers of 10-µg WFA eluates were probed with the indicated antibodies or incubated with WFA lectin (WFA). Immunoblot exposures for each antibody/lectin

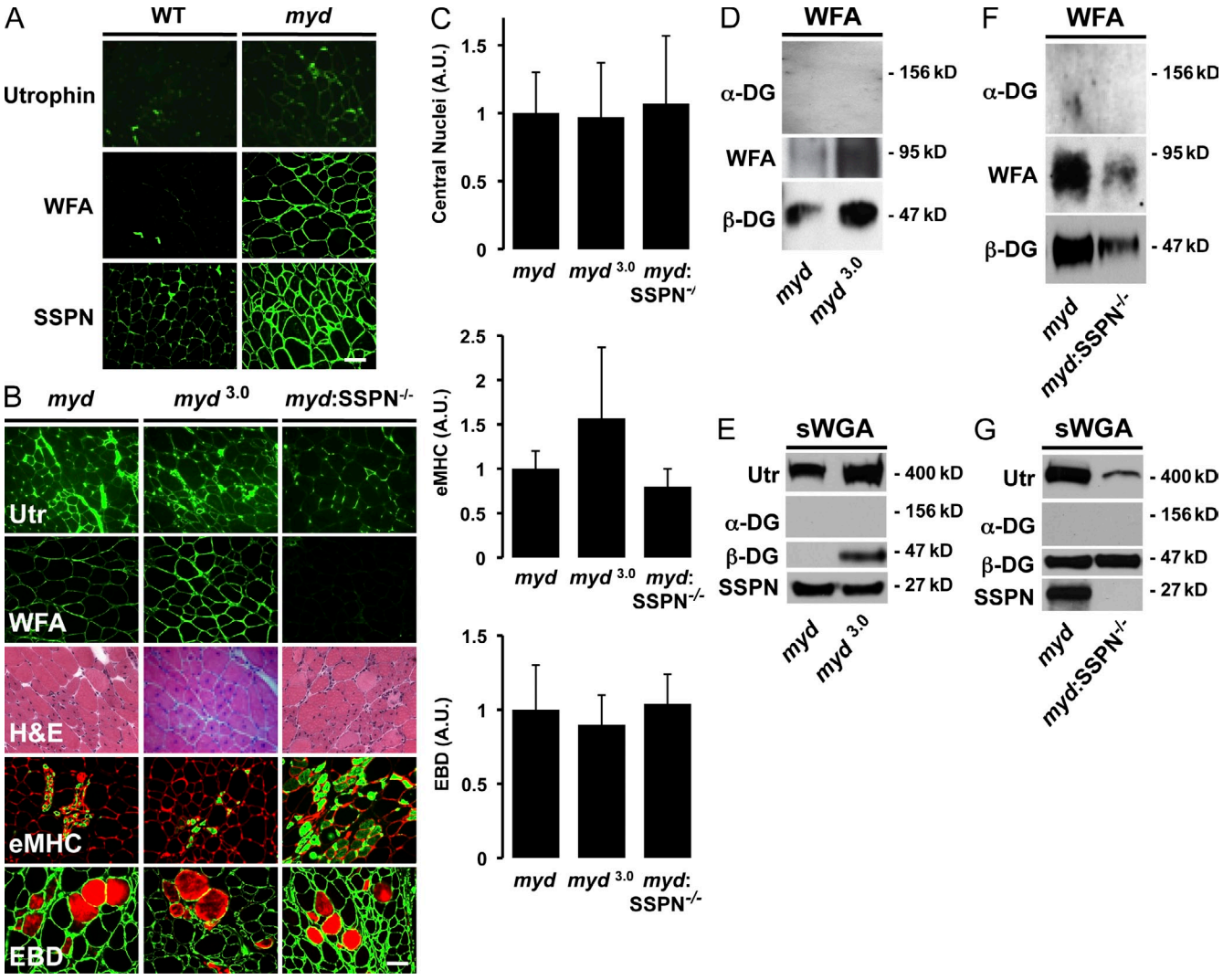

Figure 6. **SSPN regulates utrophin levels and glycosylation of α-DG in *myd* mice.** (A) Transverse cryosections of quadriceps muscles were stained with the indicated antibodies and overlayed with biotinylated WFA. (B) Transverse cryosections of quadriceps muscles were stained with indicated antibodies and overlayed with biotinylated WFA. Staining with IIH6 antibodies, which recognize LARGE epitopes on α-DG, was not detected in *myd* samples, as expected (Fig. S4). Transverse cryosections of skeletal muscle from 4–6-wk-old *myd*, SSPN-Tg:*myd* (*myd*$^{3.0}$), and SSPN-deficient *myd* (*myd*:SSPN$^{-/-}$) mice were stained with H&E. Muscle sections were stained with antibodies to embryonic myosin heavy chain (eMHC; green) as a marker for newly regenerated myofibers. Mice were injected with Evans blue dye (EBD), a marker for membrane instability (visualized by red fluorescence). Sections were costained with laminin antibodies (green fluorescence) to visualize individual fibers. (C) Quantification of central nucleation, Evans blue dye–positive fibers, and eMHC-positive fibers is expressed as a percentage of total fibers. Error bars represent standard deviation of the mean (n = 4 quadriceps per genotype). (D–G) Skeletal muscles from the indicated mice were enriched using either sWGA or WFA lectin chromatography. Immunoblots of 10-µg protein eluates are shown. A.U., arbitrary unit; Utr, utrophin. Bars, 50 µm.

of the SSPN-Tg into skeletal muscle of *myd* mice further elevates WFA binding along with broad, extrasynaptic localization of utrophin (Fig. 6 B). Using SSPN-null mice, we demonstrate that removal of SSPN from *myd* muscle reduces the level of extrasynaptic utrophin and glycosylation of α-DG, as indicated by decreased WFA binding to *myd* sarcolemma in lectin overlay assays (Fig. 6 B). Although utrophin mRNA expression is elevated 3.0-fold in *myd* muscle relative to WT controls, SSPN did not further alter utrophin transcript levels in *myd* samples (Fig. 5 E). We found that pathology of *myd* muscle was

staining are identical in Fig. 6 F, permitting direct comparisons. (C) sWGA-enriched protein samples were separated by ultracentrifugation through 5–20% sucrose gradients. Fraction numbers are indicated above the panels, where fraction 1 represents the lightest region of the gradient. Protein samples were analyzed by immunoblotting to the indicated antibodies, and exposures are identical for WT and SSPN-null fractions. (D) Quantitative RT-PCR was used to investigate whether loss of SSPN alters RNA levels of CT GalNAc transferase (*Galgt2*). Data are expressed relative to that of WT controls. Error bars represent standard deviation (n = 4 mice per genotype). (E) Skeletal muscle from WT and SSPN-deficient (SSPN$^{-/-}$) muscles were solubilized in 60 µg RIPA buffer and analyzed by immunoblots with Galgt2 antibodies. (F) Quantitative RT-PCR was used to investigate the effect of SSPN on utrophin (Utr) mRNA levels. RNA was isolated from WT, SSPN-null (SSPN$^{-/-}$), LARGE-null (*myd*), SSPN-deficient *myd* (*myd*:SSPN$^{-/-}$), and threefold SSPN-Tg:*myd* (*myd*$^{3.0}$) skeletal muscle. mRNA expression levels were normalized to GAPDH mRNA. Data are expressed relative to that of WT controls. Error bars represent standard deviation (n = 3 mice per genotype; ***, $P < 0.0001$). A.U., arbitrary unit.

unaffected by the loss of SSPN or SSPN overexpression, demonstrating that alterations in glycosylation of α-DG do not affect the absence of the laminin-binding domain on α-DG (Fig. 6, B and C). Robust expression of the DGC was detected around the sarcolemma of *myd* and SSPN-Tg:*myd* (*myd*$^{3.0}$) muscle (Fig. S4 A) and likewise in total protein immunoblots (Fig. S4 B). SSPN also increased integrin levels in *myd*$^{3.0}$ samples relative to *myd* controls (Fig. S4 B).

Analysis of WFA and sWGA enrichments demonstrates that glycosylation of α-DG and utrophin protein is increased in *myd*$^{3.0}$ muscle (Fig. 6, D and E). SSPN overexpression affects glycosylation of α-DG and utrophin expression in *myd* muscle in a manner that is similar to SSPN's effects in *mdx* muscle, but the increased GalNAc modification of α-DG is unable to compensate for the loss of LARGE glycans (Fig. 6, D and E). Furthermore, we found that absence of SSPN protein nearly abolished WFA binding of α-DG prepared from *myd*:SSPN$^{-/-}$ muscle in overlay experiments and drastically reduced the amount of β-DG associated with α-DG (Fig. 6 F). Analysis of sWGA enrichments of SSPN-deficient *myd* muscles revealed that the loss of SSPN dramatically decreases levels of utrophin associated with β-DG (Fig. 6 G) and mildly reduces sarcolemma expression of the DGC (Fig. S4 C), whereas total protein levels in input lysates did not change (Fig. S4 D). These data suggest that NMJ-specific glycosyltransferases, such as Galgt2, are able to modify α-DG in the absence of LARGE glycans on α-DG. Our data suggest that GalNAc modifications of α-DG are independent of the O-mannose–linked glycans that constitute the major laminin-binding domain on α-DG.

SSPN increases utrophin levels by activation of Akt signaling

Also known as protein kinase B, the Akt family of serine/threonine kinases is activated downstream of cell surface receptor tyrosine kinases and the phosphoinositide 3-kinase pathway. Akt induces skeletal muscle hypertrophy in vitro and in vivo through activation of the mammalian target of rapamycin pathway (Bodine et al., 2001; Rommel et al., 2001; Pallafacchina et al., 2002; Takahashi et al., 2002). As a central node in growth factor signaling, Akt activity is subject to multiple regulatory inputs. Using an inducible Akt model system, we found that Akt activation in *mdx* muscle dramatically improved membrane stability by increasing sarcolemma UGC levels (Blaauw et al., 2008, 2009; Peter et al., 2009; Kim et al., 2011).

Using immunoblot analysis of quadriceps muscle lysates, we demonstrate that increased SSPN expression in *mdx* skeletal muscle dramatically induces Ser473 phosphorylation of Akt, thereby activating Akt pathways (Fig. 7 A). Downstream p70S6K signaling, which promotes cell growth and protein translation, is activated by SSPN expression in *mdx*$^{1.5}$ muscle relative to *mdx* controls (Fig. 7 A). However, activation of GSK3β by phosphorylation was unaffected by overexpression of SSPN, suggesting that regulation of cell cycle via GSK3β pathways is not altered by SSPN (Vivanco and Sawyers, 2002). In WT mice, 1.5-fold SSPN overexpression has small, but detectable, effects on Akt signaling (Fig. 7 A). The trends in Akt activation are similar to that reported in Akt-transgenic *mdx* mice overexpressing phosphorylated Akt (*mdx*^{Akt}), supporting a role of SSPN in activating downstream signaling pathways that regulate cell growth and protein translation (Fig. S5 A; Vivanco and Sawyers, 2002; Peter et al., 2009). Using immunoblot analysis, we demonstrate that Akt signaling is significantly affected by loss of SSPN as revealed by the nearly complete absence of Akt activation in SSPN-null muscle (Fig. 7 B). Downstream phosphorylation of p70S6K is barely detectable in muscle from SSPN$^{-/-}$ samples (Fig. 7 B). Loss of SSPN does not alter total protein levels of either Akt or p70S6K, demonstrating that SSPN is an upstream activator of Akt signaling.

We previously demonstrated that Akt does not associate with the DGC (Peter and Crosbie, 2006), but the question of whether Akt interacts with the UGC, integrin, or insulin-like growth factor receptor (IGF-R) was not investigated. To address this question, we purified the UGC from *mdx* skeletal muscle lysates using sWGA lectin chromatography. Akt is not glycosylated and will only adhere to the sWGA column by direct interaction with sWGA-associated proteins. We show that the UGC, integrin, and IGF-R are enriched in eluate samples from *mdx* mice (Fig. 7 C) and are not present in void fractions (Fig. S5 B). We demonstrate that a portion of the Akt pool is present in sWGA eluates from *mdx* muscle (Fig. 7 C). The remaining Akt is present in the sWGA void and likely represents the cytosolic fraction, in agreement with data from DMD muscle (Fig. S5 B; Peter and Crosbie, 2006). Data from WT muscle is provided for comparison and demonstrates that Akt is not retained on sWGA columns, which primarily contain DGC in high quantities. We found that Akt remained associated with an sWGA-binding glycoprotein in a utrophin- and α7 integrin–independent manner (Fig. 7 C).

Newly regenerating WT myofibers in cardiotoxin (CTX)-injured muscle robustly express utrophin throughout the extrasynaptic sarcolemma (Fig. 7 D). In fact, these same fibers are also highly reactive to WFA, suggesting that the canonical GalNAc modification of α-DG enriched at NMJs in mature muscle is also present during the early stages of myofiber regeneration.

SSPN regulates Akt signaling to control utrophin expression during muscle repair

Although it is well established that newly regenerated muscle fibers express high levels of utrophin around the extrasynaptic sarcolemma (Helliwell et al., 1992; Galvagni et al., 2002; Angus et al., 2005), the dependency of muscle regeneration on utrophin and SSPN expression is unknown. The expression of utrophin during myogenic differentiation (Gramolini and Jasmin, 1999) also suggests that utrophin may be critical for complete recovery from CTX injury. Quadriceps muscles from WT and SSPN-null mice were injected with CTX to induce muscle damage and were assessed at 2, 4, 7, and 14 d after injury using four criteria (Fig. 8). Overall muscle and sarcolemma damage appeared to be identical for WT and SSPN-null samples shortly after CTX treatment (day 2), indicating that muscles were injured to a similar extent (Fig. 9 A). Signs of muscle regeneration, denoted by embryonic myosin

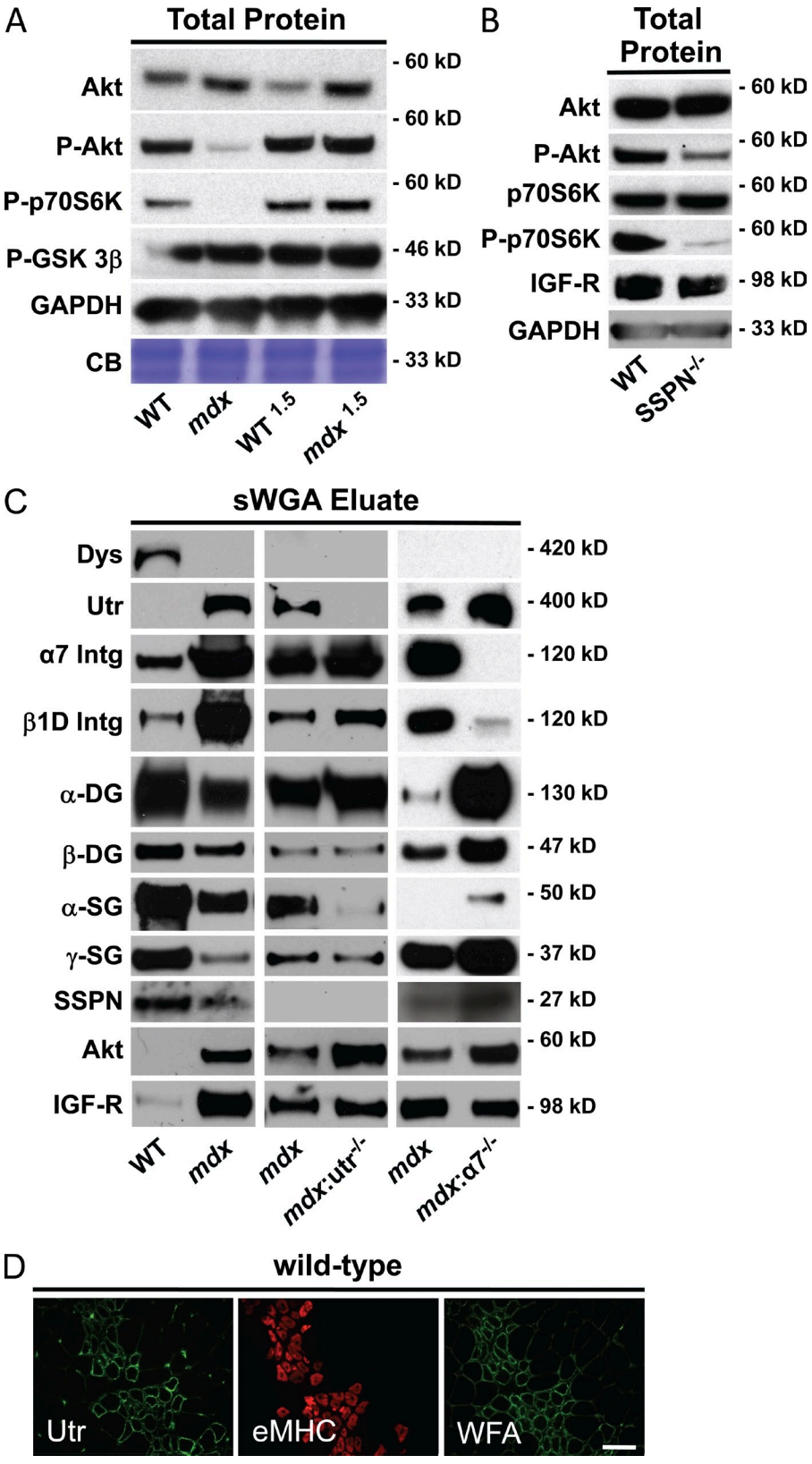

Figure 7. **SSPN is required for activation of Akt signaling.** (A) Quadriceps protein lysates were prepared in modified RIPA buffer, and 50-µg samples were analyzed by immunoblotting as shown. GAPDH and Coomassie blue (CB) staining are provided as controls for equal loading. (B) Total skeletal muscle from wild-type (WT) and SSPN-null (SSPN$^{-/-}$) mice were solubilized in modified RIPA buffer, and 60 µg of each sample was analyzed by immunoblotting with indicated antibodies. GAPDH is provided as a control for equal loading. (C) Skeletal muscle protein lysates from WT, *mdx*, utrophin-deficient *mdx* muscle (*mdx*: utr$^{-/-}$), and α7 integrin–deficient *mdx* muscle (*mdx*: α7$^{-/-}$) were enriched by sWGA lectin affinity chromatography (sWGA eluate). Immunoblots of 10-µg bound proteins eluted with GlcNAc are shown. Void (unbound) fractions are shown in Fig. S5 B. (D) WT quadriceps were injected with CTX to induce skeletal muscle degeneration/regeneration to evaluate the expression of utrophin and WFA binding without the complications of *mdx* pathology. Injected muscle cryosections were costained with utrophin (green fluorescence) and embryonic myosin heavy chain (eMHC; red fluorescence) as a marker for newly regenerated fibers 4 d after CTX injection. Serial sections were stained with WFA lectin (green fluorescence). Staining was visualized by indirect immunofluorescence. Actively regenerating myofibers displayed robust utrophin expression and WFA binding around the same nonjunctional areas of the sarcolemma. Mice were 6.5 wk of age at the time of analysis. Bar, 50 µm. Utr, utrophin; Dys, dystrophin; P, phospho; Intg, integrin.

heavy chain (eMHC)–positive myofibers with centrally placed nuclei, appeared at day 4 after injury for both genotypes (Fig. 9 A). However, SSPN-deficient muscles displayed persistent damage at day 7 and regeneration at 7 and 14 d after injury, when WT muscles start to exhibit signs of successful repair by a reduction in newly regenerating fibers (Fig. 9 A). We show that utrophin expression was increased in CTX-treated WT muscles but that SSPN-deficient muscle failed to express utrophin after CTX injury (Fig. 9 B). Furthermore, activation of Akt was evident in regenerating WT

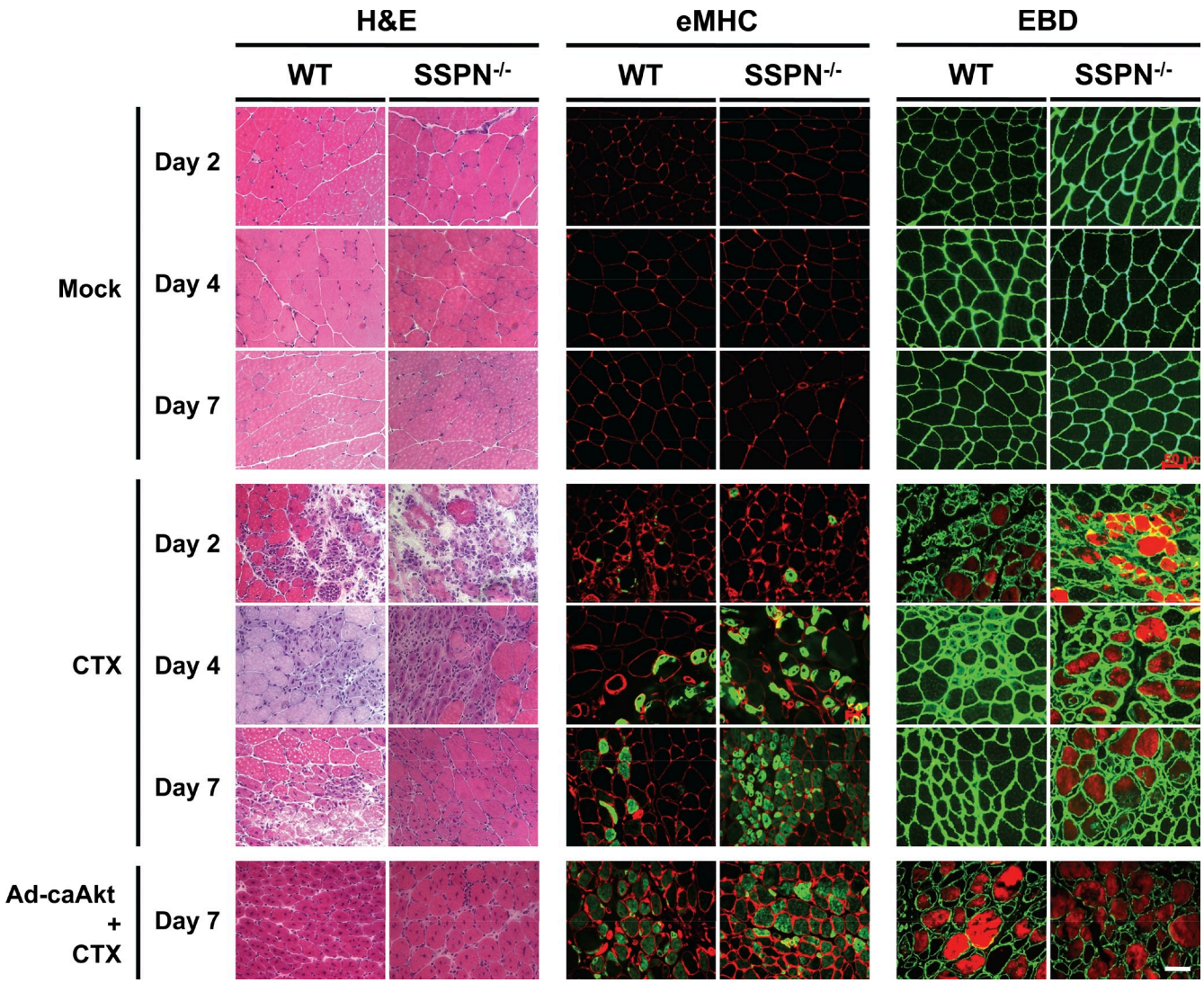

Figure 8. **Defective repair in SSPN-null muscle after injury is corrected with constitutively active Akt.** Transverse quadriceps muscle from wild type (WT) and SSPN null ($SSPN^{-/-}$) injected with cardiotoxin (CTX) and pretreated with adenovirus containing constitutively active Akt before CTX injury (Ad-caAkt + CTX) were analyzed for dystrophic pathology (H&E, eMHC, and Evans blue dye [EBD]) at 2, 4, and 7 d after injection. Significant increases in regeneration (H&E and eMHC) and membrane damage (Evans blue dye) were observed in SSPN-deficient muscle relative to WT muscle. Akt administration before CTX injury restores differences in pathology in SSPN-deficient muscle back to WT. Bar, 50 µm.

muscles, but Akt phosphorylation was defective in SSPN nulls as shown by densitometry of immunoblots (Fig. 9 B). To determine whether increasing Akt signaling in $SSPN^{-/-}$ muscle would drive utrophin expression, thereby improving recovery from muscle damage, we pretreated quadriceps muscles with adenovirus expressing constitutively active Akt (Ad-caAkt) before CTX injury, which promotes muscle growth. Activation of Akt signaling dramatically improved regeneration in SSPN-deficient muscle similar to WT (Fig. 9 C). Importantly, Ad-caAkt treatment restored utrophin expression to normal levels after CTX injury in SSPN nulls (Fig. 9 D). The specificity of the Akt response is indicated by persistent lack of dystrophin and integrin in injured $SSPN^{-/-}$ muscle pretreated with Ad-caAkt (compare Fig. 9, B and D). Our findings reveal that a novel molecular mechanism in which SSPN regulates utrophin levels in an Akt-dependent manner is required for regeneration after injury (Fig. 10).

Discussion

We provide genetic and biochemical evidence that SSPN is a major regulator of Akt signaling, utrophin expression, and glycosylation of α-DG in skeletal muscle. Using transgenic overexpression models, we show that increasing SSPN results in a concomitant increase in utrophin, dystrophin, and α7β1 integrin around the extrasynaptic sarcolemma (Fig. 10). Furthermore, we use SSPN-null mice to demonstrate that loss of SSPN dramatically reduces utrophin association with its glycoprotein complex, supporting an important role of SSPN in maintaining structural integrity within the UGC. We provide the first biochemical data to demonstrate that SSPN is a significant determinant of glycosylation by regulating Galgt2 protein levels in the ER/Golgi. We demonstrate that SSPN-induced improvements in cell surface expression of α-DG result in increased laminin binding (Fig. 10). Loss of

SSPN in WT mice impairs Akt signaling and decreases utrophin levels at the cell surface, whereas utrophin is increased in ER/Golgi. Our data demonstrate that SSPN is an important component of the utrophin-based compensatory mechanism in *mdx* mice.

SSPN forms complex interactions with neighboring SSPN proteins to form higher order structures that, like many tetraspanins, promote protein interactions within the membrane bilayer (Miller et al., 2007). Intramolecular disulfide cross-linking of cysteines within the large extracellular loop between transmembrane domains 3 and 4 is critical for formation of the SG–SSPN subcomplex (Miller et al., 2007). In support of this role, loss of tetraspanin expression has been shown to negatively affect cell surface expression of tetraspanin-associated integrins (Charrin et al., 2009). We provide the first evidence that SSPN affects transportation of utrophin–DG adhesion complexes in skeletal muscle. Conversely, loss of SSPN in *mdx* muscle increases the levels of utrophin and WFA-binding DG in the ER/Golgi, preventing the transport of these complexes to the sarcolemma. We demonstrate that N-terminal fragments of dystrophin, produced from the *mdx* premature termination codon, accumulate in the ER/Golgi compartments. These truncated dystrophin proteins are not transported to the cell surface, likely because of misfolding within the ER/Golgi. These findings raise the question of whether improper dystrophin folding during protein processing elicits ER stress, resulting in the unfolded protein response, which would be consistent with mislocalization of ER/Golgi compartments in *mdx* skeletal muscle (Percival et al., 2007).

We demonstrate that SSPN-null mice are deficient in their molecular and physiological responses to CTX induced muscle injury. SSPN-nulls are deficient in Akt signaling and utrophin expression, which we show are necessary for successful repair of damaged muscle fibers. Introduction of activated Akt into SSPN-deficient muscle rescues these molecular defects as observed by normalized expression of utrophin and effective muscle repair. We provide the first evidence that SSPN has multiple roles at the cell surface and within intracellular membrane compartments. Our results support a critical role of SSPN in UGC structure and reveal new functions for SSPN-Akt-utrophin in effective repair and regeneration after muscle injury.

SSPN is unique in that it improves expression of the three major compensatory adhesion complexes in skeletal muscle. SSPN offers many advantages over current therapeutic strategies to improve utrophin levels and laminin binding. The SSPN cDNA is very small and can be easily packaged into adeno-associated viral vectors for systemic delivery. In addition, SSPN is ubiquitously expressed in nonmuscle tissue and at low levels in dystrophin deficiency, suggesting that SSPN treatment is unlikely to pose an undesirable immune response, which has thwarted other viral-based approaches using dystrophin or utrophin. Our study has addressed the mechanistic targets of SSPN in muscle, which will facilitate future studies in developing SSPN as a therapeutic approach to the treatment of muscular dystrophy.

Materials and methods

Animal models

mdx and *myd* female breeders were purchased from Jackson ImmunoResearch Laboratories, Inc. Genotyping information is available from Jackson ImmunoResearch Laboratories, Inc. Transgenic constructs were engineered with the human skeletal actin promoter and VP1 intron (pBSX-HSAvpA expression vector) upstream of the full-length human SSPN ORF (available from GenBank/EMBL/DDBJ under accession no. AF016028) as described previously (Peter et al., 2007). Three lines were obtained from the University of California, Irvine Transgenic Mouse Facility: 0.5 SSPN-Tg, 1.5 SSPN-Tg, and 3.0 SSPN-Tg, which express ∼0.5-, 1.5-, and 3.0-fold levels of exogenous SSPN relative to endogenous SSPN levels. Transgenic mice were generated by microinjections of Tg DNA into the pronucleus of fertilized single-cell embryos (Transgenic Mouse Facility, University of California, Irvine). Males from each line were crossed to *mdx* heterozygous females to generate 0.5 SSPN-Tg:*mdx*, 1.5 SSPN-Tg:*mdx*, and 3.0 SSPN-Tg:*mdx* male mice. WT non-Tg, *mdx*, and SSPN-Tg littermates were used as controls. Males from each line were crossed to *myd* homozygous females, and the male and female progeny were crossed again to generate 0.5 SSPN-Tg:*myd*, 1.5 SSPN-Tg:*myd*, and 3.0 SSPN-Tg:*myd* mice. Wild-type non-Tg, *myd*, and SSPN-Tg littermates were used as controls. All mice were analyzed at 4–12 wk of age.

SSPN-deficient mice were a gift from K.P. Campbell (University of Iowa Medical School, Howard Hughes Medical Institute, Iowa City, IA; Lebakken et al., 2000). The SSPN-deficient embryonic stem cells were engineered by homologous recombination to lack a 7.6-kb fragment of DNA, which included 233 bp of intron 1, exon 2, and intron 2 and 1.8 kb of exon 3 (the entire coding region of exon 3). Genotypes were confirmed with the following oligonucleotide primers: SPNI1FA, 5′-ACTCCCTGGAATACAGAGGAACT-3′; SPNI2RA, 5′-TACAAGGGGACAGACACTCAGAC-3′; and neomycin-SSPN knockout, 5′-TTTCTCTTGATTCCCACTTTGTG-3′. PCR conditions were as follows: denaturation at 94°C for 2 min followed by 35 cycles of 1 min at 94°C, 1 min at 55°C, and 1.5 min at 72°C. SSPN-null males were crossed to *mdx* homozygous females. The resulting *mdx* heterozygous, SSPN heterozygous females were mated to SSPN heterozygous males to generate WT, SSPN-null, *mdx*, and *mdx*:SSPN-null males, which were analyzed at 3 wk of age. The identical crosses were performed with *myd* mice to generate WT, SSPN-null, *myd*, and *myd*:SSPN-null males that were analyzed at 4 wk of age. α7 integrin–deficient mice were a gift from D.J. Burkin (transferred from University of Nevada [Reno, NV] to University of California, Los Angeles [Los Angeles, CA]) and crossed with *mdx* mice as previously described (Rooney et al., 2006). The α7 integrin–deficient mice were created by replacing exon 1 of the α7 integrin gene with the lactose operon Z/neomycin cassette to permit expression of the β-galactosidase reporter gene from the α7 integrin promoter. Genotypes were confirmed with the following primers: α7PF10, 5′-TGAAGGAATGAGTGCACAGTGC-3′; α7exon1R1, 5′-AGATGCCTGTGGGCAGAGTAC-3′; and bgalR2, 5′-GACCTGCAGGCATGCAAGC-3′. The following cycling conditions were used: α7 WT band denaturation at 95°C for 4 min followed by 35 cycles of 1 min at 95°C, 1 min at 62°C, and 2 min at 72°C and α7-null band denaturation at 95°C for 4 min followed by 35 cycles of 1 min at 95°C, 1 min at 57.5°C, and 1 min at 72°C. Tissue was harvested at 3 wk of age. *mdx*:utrophin-null mice were a gift from J. Sanes (Harvard University, Cambridge, MA) and sent from the mouse colony of J. Chamberlain (University of Washington, Seattle, WA). Utrophin-null mice were generated with 137-bp deletion corresponding to bp 8,624–8,787 of the utrophin gene. The following primers and cycling conditions were used to confirm genotypes: (forward) constant, 5′-CTGAGTCAAACAGCTTGGAAGCCTCC-3′; (reverse) WT, 5′-TTGCAGTGTCTCCCAATAAGGTATGA-3′; (reverse) mutant, 5′-TGCCAAGTTCTAATTCCATCAGAAGCTG-3′; and denaturation at 95°C for 5 min followed by 40 cycles of 1 min at 95°C, 1 min at 65°C, and 1 min at 72°C. Tissues were harvested at 6 wk of age.

Akt transgenic mice (Izumiya et al., 2008) were a gift from K. Walsh (Boston University, Boston, MA) and crossed with *mdx* mice as previously described (Peter et al., 2009). Transgenic HA-tagged mouse myrAkt1 mice were created by pronuclear injection. Double transgenic mice were created by breeding tetracycline response element–myrAkt1 transgenic mice harboring the constitutively active form of mouse Akt1 controlled by the tetracycline-responsive promoter with muscle creatine kinase (MCK)–reverse tetracycline transactivator (rtTA) transgenic mice expressing the tetracycline transactivator controlled by a mutated skeletal MCK promoter. Single transgenic mice were used and treated with doxycycline as controls. Activation of the Akt-Tg was accomplished by

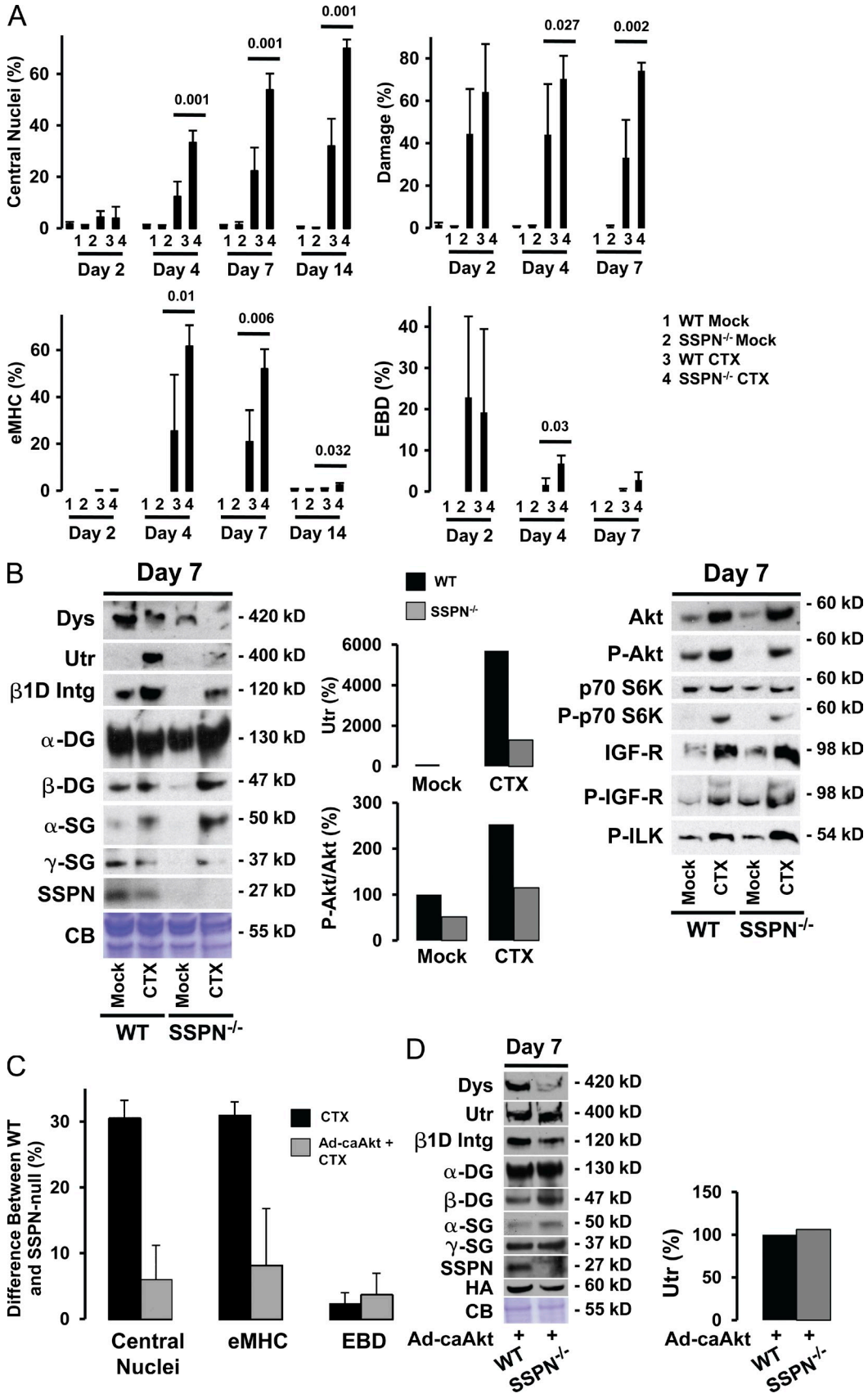

Figure 9. **Akt restores utrophin and rescues impaired regeneration in SSPN-deficient muscle after CTX injury.** (A) Transverse quadriceps muscles from wild type (WT) and SSPN null ($SSPN^{-/-}$) injected with mock and cardiotoxin (CTX) were quantified for regeneration (central nuclei and eMHC), membrane damage (Evans blue dye [EBD]), and total area of damage (damage). The postinjection time points are indicated. Error bars represent standard deviation. P-values are provided in each plot (n = 4 quadriceps per treatment per genotype). (B) Skeletal muscle protein lysates were prepared in IP buffer from

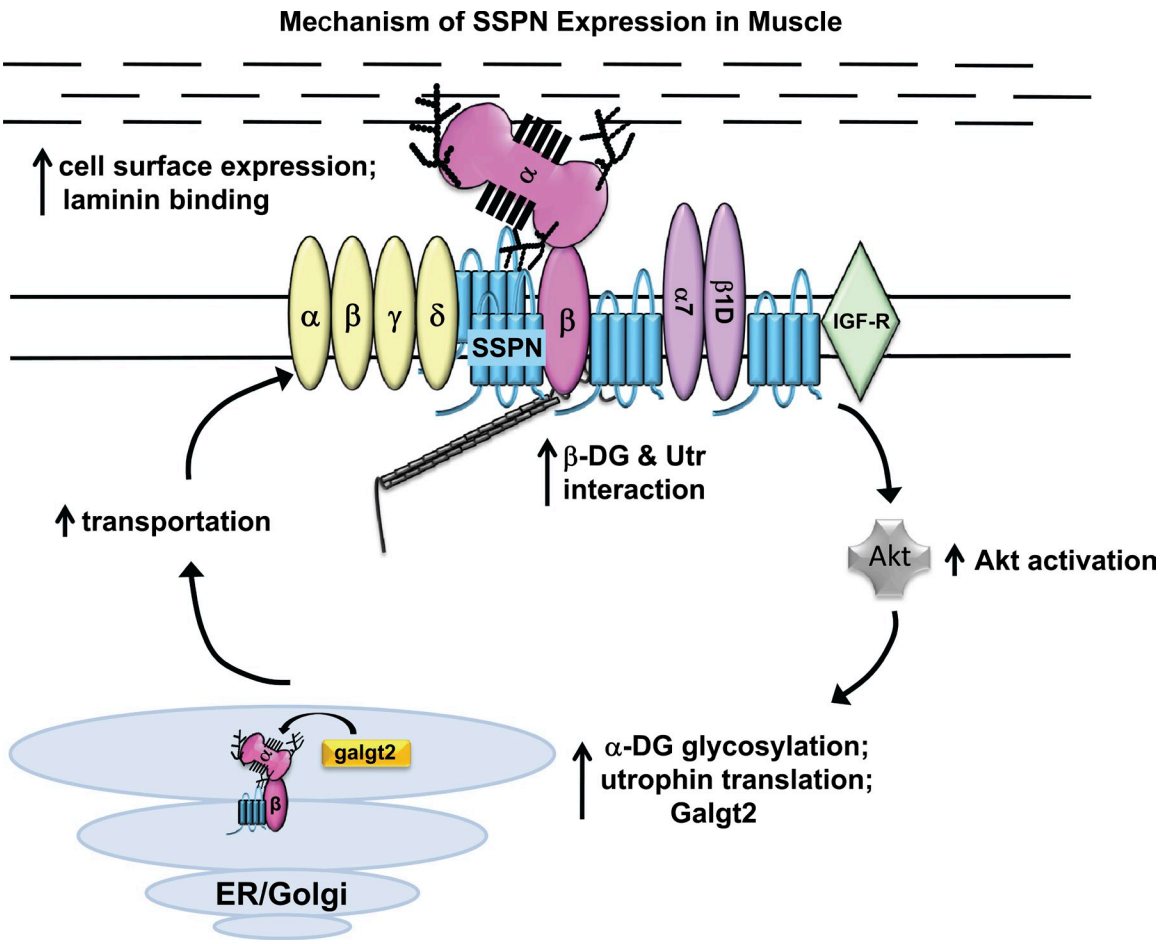

Figure 10. **Molecular mechanisms of SSPN action at the cell surface and in protein processing.** DGs (pink), SGs (yellow), SSPN (blue), integrins (purple), IGF-R (green), and Akt (gray) are shown. Utrophin (Utr) is depicted in gray. Overexpression of SSPN in *mdx* muscle elicits a series of molecular events that lead to restoration of laminin binding and rescue of *mdx* pathology. SSPN activates Akt, leading to increased utrophin and integrin abundance. SSPN increases Galgt2 in the ER/Golgi membranes that facilitate increased CT antigen modification of α-DG. SSPN enhances transportation of utrophin-DG at the sarcolemma and restores laminin binding and membrane stability.

treating 3-wk-old mice for 3 wk with 0.5 mg/ml doxycycline (Peter et al., 2009). The tetracycline response element–myrAkt1-Tg was amplified using the following primers: Tet-Akt #1, 5′-CTGGACTACTTGCACTCCGAGAAG-3′; and Tet-Akt #2, 5′-CTGTGTAGGGTCCTTCTTGAGCAG-3′. PCR conditions were denaturation at 95°C for 5 min followed by 30 cycles of 30 s at 95°C, 30 s at 68°C, and 1 min at 72°C. PCR amplifications of the MCK-rtTA-Tg was amplified using the following primers: MCK-rtTA #1, 5′-CATCTGCGGACTGGAAAAACAAC-3′; and MCK-rtTA #2, 5′-GCATCGGTAAACATCTGCTCAAAC-3′. PCR conditions were denaturation at 95°C for 5 min followed by 30 cycles of 30 s at 95°C, 30 s at 62°C, and 1 min at 72°C. Quadriceps muscles from female Akt S-Tg (WT single transgenic) and Akt D-Tg (WT double transgenic) and male Akt S-Tg:*mdx* and Akt D-Tg:*mdx* littermates were harvested from mice at 6 wk of age. Mice were maintained in the Life Sciences Vivarium, and all procedures were performed in accordance with guidelines set by the University of California, Los Angeles Institutional Animal Care and Use Committee.

Evans blue dye assay

Sarcolemma membrane damage was assessed using an Evans blue dye tracer analysis that was performed by an intraperitoneal injection of mice with 50 µl Evans blue dye (10 mg/ml in 10 mM sterile phosphate buffer and 150 mM NaCl, pH 7.4) per 10 g of body weight ≥8 h before dissection as described previously (Straub et al., 1997). Quadriceps muscles were processed as described in the next section. The percentage of Evans blue dye–positive fibers was obtained by counting the number of Evans blue dye–positive fibers in a whole quadriceps section and dividing by the total number of myofibers. Evans blue dye fibers

quadriceps of WT and SSPN-deficient muscles after CTX injury (day 7). 50-µg samples were resolved by SDS-PAGE, and immunoblots were probed with the indicated antibodies. Coomassie Blue (CB) was used for equal loading. Quantitation of phospho (P)-Akt and Akt immunoblots was performed using densitometry, and data are represented as a ratio of phospho-Akt to Akt normalized to WT controls (100%). Similarly, densitometry of utrophin levels was normalized to WT controls (100%). The data shown are from a single representative experiment out of three repeats from separate mice. (C) Dystrophic pathology was quantified from transverse quadriceps sections of WT and SSPN deficient ($SSPN^{-/-}$) injured with CTX and pretreated with adenovirus containing constitutively active Akt before CTX injury (Ad-caAkt + CTX). Data are represented as the difference in means between WT and $SSPN^{-/-}$ for central nucleation, eMHC, and Evans blue dye at day 7. Error bars represent standard deviation (n = 3–4 quadriceps per genotype). (D) Total protein was isolated in IP from mice pretreated with Ad-caAkt and injured with CTX. Equal concentrations (50 µg) were loaded on SDS-PAGE and transferred to nitrocellulose membranes. Immunoblotting was performed with the antibodies indicated. Akt expression from Ad-caAkt was detected using antibodies against the HA tag that were engineered onto the caAkt construct (HA). Coomassie blue was used for equal loading. Densitometry was used to quantify utrophin protein levels from immunoblots. Data shown are relative to WT Ad-caAkt–treated CTX-injured muscle analyzed at day 7 (100%). The data shown are from a single representative experiment out of three repeats from separate mice. Utr, utrophin; Intg, integrin.

fluoresce red in the microscope, and a counter stain with laminin delineates the outline of all myofibers.

Immunofluorescence and lectin overlay assays

Muscles were mounted in 10.2% polyvinyl alcohol/4.3% polyethylene glycol and flash frozen in liquid nitrogen–cooled isopentane. Muscles were stored in −80°C until further processing. 8-µm transverse sections were placed onto positively charged glass slides (Thermo Fisher Scientific) and stored at −80°C. Sections were acclimated to RT for 15 min and blocked with 3% BSA diluted in PBS for 30 min at RT. The avidin/biotin blocking kit (Vector Laboratories) was used according to manufacturer's instructions. Mouse primary antibodies were prepared with the Mouse on Mouse blocking reagent (Vector Laboratories) as described by the manufacturer's protocol. Sections were incubated in primary antibody in PBS at 4°C overnight with the following antibodies or lectin: dystrophin (MANDYS1; 1:5; Development Studies Hybridoma Bank), utrophin (MANCHO3, 1:5; Development Studies Hybridoma Bank), β-DG (MANDAG2; 1:50; Development Studies Hybridoma Bank), α-SG (VP-A105; 1:30; Vector Laboratories), β-SG (VP-B206; 1:30; Vector Laboratories), laminin (L9393; 1:25; Sigma-Aldrich), β1D integrin (MAB1900; 1:20; Millipore), human SSPN (affinity purified rabbit 15; 1:25), eMHC (F1.652; 1:25; Development Studies Hybridoma Bank), α-bungarotoxin conjugated to Alexa Fluor 555 (B35451; 1:200; Invitrogen), and WFA (B-1355; 1:500; Vector Laboratories). Polyclonal antibodies to detect exogenous (human) SSPN (SSPN aa 4–26; available from GenBank/EMBL/DDBJ under accession no. AF016028) and mouse SSPN (SSPN aa 1–26; GenBank accession no. U02487) were made by injecting rabbits separately with GST-mouse SSPN fusion protein or human SSPN peptide and affinity purified from rabbit serum (Peter et al., 2007). Primary antibodies were detected by biotinylated anti–rabbit (BA-1000; 1:500; Vector Laboratories) and biotinylated anti–mouse (BA-9200; 1:500; Vector Laboratories). Fluorescein (A-2001; 1:500; Vector Laboratories)- or Texas red (A-2006; 1:500; Vector Laboratories)–conjugated avidin D was used to detect secondary antibodies and biotinylated WFA. Both secondary and tertiary probes were diluted in PBS and incubated with sections for 1 h at RT. Sections were mounted in VECTASHIELD (Vector Laboratories) to prevent photobleaching. Sections were incubated with secondary and tertiary antibodies alone as a control for specificity. Antibody-stained sections were visualized using a fluorescent microscope (Axioplan 2; Carl Zeiss) equipped with a Plan Neofluar 40×, NA 1.3 oil differential interference contrast objective at RT, and images were captured under identical conditions using a digital color camera (AxioCam) and AxioVision Rel 4.5 software (Carl Zeiss). ImageJ software (National Institutes of Health) was used to merge all images with double labeling.

Histology

H&E staining was used for visualization of centrally placed nuclei as described previously (Peter and Crosbie, 2006). 8-µm transverse quadriceps sections were acclimated to RT for 15 min before beginning the staining procedure. Slides were incubated in hematoxylin for 5 min, washed in water for 2 min, incubated in eosin for 5 min, and dehydrated in 70, 80, 90, and 100% ethanol. Sections were then incubated in xylene for 10 min and mounted in Permount. All supplies for this procedure were purchased from Thermo Fisher Scientific. Whole quadriceps pictures were captured under identical conditions using a fluorescent microscope (Axioplan 2) and Axiovision Rel 4.5 software. The percentage of centrally nucleated fibers was assessed from six quadriceps of each genotype. The data are represented as a mean percentage of the total number of fibers in each whole quadriceps section.

Protein preparation from skeletal muscle

Total skeletal muscle was snap frozen in liquid nitrogen and stored at −80°C. For signaling blots, only quadriceps muscles were used. Tissues were ground to a fine powder using a mortar and pestle and then added to ice-cold radioimmunoprecipitation assay (RIPA; Thermo Fisher Scientific), modified RIPA (50 mM sodium fluoride, 1 mM sodium orthovanadate, 100 nM okadaic acid, and 5 nM microcystin-L-arginine), immunoprecipitation (IP) buffer (Thermo Fisher Scientific), or standard DGC buffer with 0.1% digitonin (Peter et al., 2008) with protease inhibitors (0.6 µg/ml pepstatin A, 0.5 µg/ml aprotinin, 0.5 µg/ml leupeptin, 0.75 mM benzamidine, 0.2 mM PMSF, 5 µM calpain I, and 5 µM calpeptin). Homogenates were rotated at 4°C for 1 h. Lysates were clarified by centrifugation at 15,000 rpm for 20 min at 4°C, protein concentration was determined using the DC Protein Assay (Bio-Rad Laboratories), and lysates were stored at −80°C.

Immunoblot analysis

Equal quantities (30, 50, and 60 µg) of protein samples were resolved on 4–20% precise protein gels (Thermo Fisher Scientific) by SDS-PAGE and transferred to nitrocellulose membranes (Millipore). An identical protein gel was stained with Coomassie blue stain to visualize total protein. 5% blotto (nonfat dry milk [Carnation] in TBS with 0.2% Tween 20 [Thermo Fisher Scientific]) was used to block membranes for 30 min at RT and incubate in primary antibodies overnight at 4°C. Incubations were performed with the following primary antibodies: dystrophin (MANDYS1; 1:2), utrophin (MANCHO3; 1:50), α-DG IIH6 (sc-53987; 1:500; Santa Cruz Biotechnology, Inc.), β-DG (MANDAG2; 1:250), α-SG (VP-A105; 1:100), β-SG (VP-B206; 1:100), γ-SG (VP-G803; 1:100), laminin (L9393; 1:5,000), β1D integrin (MAB1900; 1:100), α7A integrin (gift from D.J. Burkin; affinity-purified rabbit A2 345; 1:500), agrin (ab12358; 1:500; Abcam), plectin-1 (sc-33649; 1:200; Santa Cruz Biotechnology, Inc.), human SSPN (affinity-purified rabbit 15; 1:500), SSPN (affinity-purified rabbit 3; 1:5), Akt (9272; 1:750; Cell Signaling Technology), phospho-Akt (Ser473; 9271; 1:750; Cell Signaling Technology), p70S6K (9202; 1:250; Cell Signaling Technology), phospho-p70S6K (Thr389; 9336; 1:500; Cell Signaling Technology), phospho-GSK3β (Ser9; 9272; 1:750; Cell Signaling Technology), IGF-R (3027; 1:750; Cell Signaling Technology), phospho–IGF-R (3024; 1:1,000; Cell Signaling Technology), phospho–integrin-linked kinase (AB1076; 1:1,000; Millipore), Galgt2 (gift from P.T. Martin; 1:2,000; CT68 affinity-purified rabbit antiserum to KLRMKYFQDAYNQKD), CT2 (gift from P.T. Martin; 1:2; mouse IgM monoclonal antibody), HA (Biot-101L; 1:500; Covance), and glyceraldehyde 3-phosphate dehydrogenase (GAPDH; MAB374, 1:20,000; Millipore). Horseradish peroxidase–conjugated anti–rabbit IgG (GE Healthcare), anti–mouse IgG (GE Healthcare), anti–mouse IgM (Roche), and anti–goat IgG (Santa Cruz Biotechnology, Inc.) secondary antibodies were used at 1:2,000 dilutions in 5% blotto and incubated at RT for 3 h. Immunoblots were developed using enhanced chemiluminescence (SuperSignal West Pico Chemiluminescent Substrate; Thermo Fisher Scientific). Densitometry was quantified using an Alphaimager 2200 (Alpha Innotech). Autorads were exposed to white light, and the protein of interest was boxed. The same area was used for all blots from the same experiment for consistency. The mean integrated density value was recorded and normalized to controls.

sWGA and WFA enrichment of protein lysates

3.5-mg protein samples were incubated with 1.2 ml sWGA-conjugated agarose slurry (AL-1023S; Vector laboratories) or WFA-conjugated agarose slurry (AL-1353; Vector Laboratories) and gently rotated overnight at 4°C. sWGA and WFA agarose was washed four times in RIPA or standard DGC buffer (Peter et al., 2008) containing fresh protease inhibitors (0.6 µg/ml pepstatin A, 0.5 µg/ml aprotinin, 0.5 µg/ml leupeptin, 0.75 mM benzamidine, 0.2 mM PMSF, 5 µM calpain I, and 5 µM calpeptin) to remove unbound proteins. Bound proteins were eluted with 0.3 M GlcNAc (sWGA) or 0.3 M GalNAc (WFA; Sigma-Aldrich) and concentrated using filtration columns (Centricon Ultracel; Millipore) by centrifugation at 4,000 *g* for 20 min. Protein concentration was determined with the DC Protein Assay. Equal concentrations of eluates (10 µg) were resolved by SDS-PAGE and transferred to nitrocellulose membranes as described in the Immunoblot analysis section. Membranes were blocked with 5% blotto or 2% gelatin for 30 min and incubated in primary antibody diluted in 5% blotto or TBS with 0.2% Tween 20 and rocked overnight at 4°C. Immunoblotting was performed as described in the Immunoblot analysis section. All immunoblots were developed using enhanced chemiluminescence (SuperSignal West Pico Chemiluminescent Substrate).

Sucrose gradient ultracentrifugation

Protein preparation was performed as described in the Protein preparation from skeletal muscle section in IP lysis buffer (Thermo Fisher Scientific). The integrity of the UGC was determined by subjecting equal concentrations of sWGA eluates over 5–20% sucrose gradient ultracentrifugation. Gradients were mixed using the Gradient IP station (Biocomp), and sucrose gradients were centrifuged at 35,000 *g* in an ultracentrifuge (Optima L-90K; Beckman Coulter). 12 1-ml fractions were collected using the Gradient IP station and concentrated to 150 µl with centrifugal filters (Amicon Ultra; Millipore; Peter et al., 2008). Equal volumes of each fraction were resolved, transferred, and immunoblotted as described in the Immunoblot analysis section.

Laminin overlay assay

Membranes were prepared as described in sWGA and WFA enrichment of protein lysates. Membranes were blocked with 5% BSA in laminin-binding buffer (10 mM triethanolamine, 140 mM NaCl, 1 mM $MgCl_2$, and 1 mM $CaCl_2$, pH 7.6) followed by incubation of mouse ultrapure

Engelbreth-Holm-Swarm laminin (354239; BD) in laminin-binding buffer for 6 h at 4°C. Membranes were washed and incubated with rabbit anti-laminin (L9393; 1:5,000; Sigma-Aldrich) overnight at 4°C followed by horseradish peroxidase–conjugated anti–rabbit IgG or anti–mouse IgG (GE Healthcare) at RT for 3 h. Blots were developed by enhanced chemiluminescence (SuperSignal West Pico Chemiluminescent Substrate).

Quantitative RT-PCR

The RNeasy fibrous tissue kit (QIAGEN) was used according to the manufacturer's instructions to isolate total RNA from gluteus maximus or quadriceps of 3–6-wk-old mice. Dissected muscles were stored in RNA*later* (Invitrogen). RNA integrity was verified by visualization of RNA after electrophoresis through agarose. RNA concentrations were determined using a spectrophotometer (NanoDrop 1000; Thermo Fisher Scientific). Reverse transcription was performed using SuperScript III (Invitrogen) or Maxima First Strand cDNA Synthesis kit (Fermentas) with 3 µg of total RNA following the recommendations of the manufacturer. Quantitative real-time PCR was performed in triplicates on a TaqMan ABI PRISM 7900 (Applied Biosystems). PCR reaction mix for Galgt2 and the 18S ribosome consisted of a primer–probe mix, TaqMan Universal PCR master mix with AmpliTaq Gold DNA polymerase (Applied Biosystems), uracil-*N*-glycosylase (AmpErase; Applied Biosystems), deoxyribonucleotide triphosphates with deoxy-UTP, and a passive reference to minimize background fluorescence fluctuations (product no. 4304437; Applied Biosystems). After an initial hold of 2 min at 50°C to allow activation of AmpErase and 10 min at 95°C to activate the AmpliTaq polymerase, the samples were cycled 40 times at 95°C for 15 s and 60°C for 1 min.

Primers and probe against CT GalNAc transferase were custom made by Applied Biosystems and provided as a 20× reaction mix containing 18 µmol/liter each of primers (forward primer sequence, 5′-GATGTCCTGGAGAAAACCGAACT-3′; and reverse primer sequence, 5′-GCAGCCTGAACTGGTAAGTATTCC-3′) and 5 µmol/liter of probe (probe sequence, 5′-CCGCCCACCACATCC-3′). 18S ribosomal RNA probe contained VIC dye as the reporter, whereas all other probes had 6-carboxyfluorescein reporter dye at the 5′ end (Xu et al., 2007a,b). GAPDH mRNA (utrophin) and 18S ribosomal RNA (CT GalNAc transferase; 4308329; Applied Biosystems) were used as internal controls. The SYBR green quantitative PCR master mix (Maxima; Fermentas) was used for the utrophin and GAPDH reactions. GAPDH was specifically amplified using GAPDH forward (5′-ACTCCACTCACGGCAAATTC-3′) and GAPDH reverse (5′-TCTCCATGGTGGTGAAGACA-3′) primers, which specifically amplified a 171-bp target sequence in mouse GAPDH cDNA. Utrophin cDNA was amplified using utrophin forward (5′-GGGGAAGATGTGAGAGATTT-3′) and utrophin reverse (5′-GTGTGGTGAGGAGATACGAT-3′) primers, which specifically amplified a 548-bp target of the mouse utrophin (Jasmin et al., 1995; Peter et al., 2008). Cycling conditions were 95°C for 10 min followed by 40 cycles of 15 s at 95°C and 60 s at 60°C with data acquisition performed during the annealing/extension step, and relative gene expression was quantified by the $2^{-\Delta\Delta CT}$ method. Student's *t* test was used for statistical analysis of significance.

ER/Golgi preps

ER/Golgi enrichments of total skeletal muscle were performed with the Endoplasmic Reticulum Enrichment kit (IMGENEX Corporation) according to instructions provided by the manufacturer. 50 µg of enrichments from WT, 1.5-fold SSPN-Tg, *mdx*, 1.5-fold SSPN-Tg:*mdx*, 3.0-fold SSPN-Tg:*mdx*, and *mdx*:SSPN-null muscle were separated by SDS-PAGE and transferred to nitrocellulose membranes as described in the Immunoblot analysis section. Immunoblotting was performed as described previously with the addition of antibodies against ER and Golgi markers: ATF6 (IMG-273; 1:100; IMGENEX Corporation) and GM130 (G7295; 1:1,000; Sigma-Aldrich).

CTX injury model and adenovirus injection

At 6 wk of age, the left quadriceps muscle of WT and SSPN-null male mice was injected with 200 µl of 10-µM CTX from *Naja nigricollis* (EMD) in PBS. An identical volume of PBS was injected into the contralateral quadriceps as a control. Quadriceps muscles were collected 2, 4, 7, and 14 d after injection. Mice treated with adenovirus containing constitutively active Akt (Ad-caAkt) were injected with 3.3×10^8 particle-forming units 48 h before CTX injury.

Online supplemental material

Fig. S1 contains immunofluorescence data for the SGs and DG on non-transgenic compared with transgenic mice on the WT and *mdx* background and total protein immunoblots for the adhesion complexes. Fig. S2 contains WFA overlays on WT and *mdx* mice. Fig. S3 contains immunofluorescence data in WT and SSPN-deficient mice. Fig. S4 contains immunofluorescence data and total protein immunoblots for the adhesion complexes in *myd*, SSPN transgenic *myd*, and SSPN-deficient *myd* mice. Fig. S5 contains immunoblot data for the Akt signaling in Akt transgenic mice and sWGA voids (unbound lysates) of WT, *mdx*, utrophin-deficient *mdx*, and α7 integrin–deficient *mdx* mice. Online supplemental material is available at http://www.jcb.org/cgi/content/full/jcb.201110032/DC1.

The authors thank M. Cross, N.J. Hsu, M.P. Huang, A. Iyengar, C. Ko, A. Kwok, G. Miller, M. Song, and R. Spence (University of California, Los Angeles, Los Angeles, CA) for technical assistance, Dr. T. Kitada for critically reading the manuscript, Dr. Linda Baum for helpful discussions, Dr. D.J. Burkin for sending the *mdx*:$\alpha7^{-/-}$ mice from his colony, and Dr. J. Chamberlain for sending the *mdx*:utr$^{-/-}$ mice from his colony.

This work was supported by grants from the Genetic Mechanisms Predoctoral Training Fellowship US Public Health Service National Research Service Award (GM07104), Edith Hyde Fellowship, and the Eureka Fellowship to J.L. Marshall; Tegger Foundation and Swedish Research Council (524-2009-619) to J. Holmberg; Undergraduate Research Fellows Program to E. Chou; the Molecular, Cellular, and Integrative Physiology Predoctoral Training Fellowship (T32 GM65823), Edith Hyde Fellowship, Ursula Mandel Fellowship, Harold and Lillian Kraus American Heart Association Predoctoral Fellowship to A.K. Peter; National Institutes of Health/National Institute of Arthritis and Musculoskeletal and Skin Diseases (NIAMS; R01 AR047922) to P.T. Martin; and National Institutes of Health/NIAMS (R01 AR048179 and P30 AR057230) to R.H. Crosbie-Watson.

Submitted: 7 October 2011
Accepted: 24 May 2012

References

Allamand, V., and K.P. Campbell. 2000. Animal models for muscular dystrophy: valuable tools for the development of therapies. *Hum. Mol. Genet.* 9:2459–2467. http://dx.doi.org/10.1093/hmg/9.16.2459

Angus, L.M., J.V. Chakkalakal, A. Méjat, J.K. Eibl, G. Bélanger, L.A. Megeney, E.R. Chin, L. Schaeffer, R.N. Michel, and B.J. Jasmin. 2005. Calcineurin-NFAT signaling, together with GABP and peroxisome PGC-1alpha, drives utrophin gene expression at the neuromuscular junction. *Am. J. Physiol. Cell Physiol.* 289:C908–C917. http://dx.doi.org/10.1152/ajpcell.00196.2005

Blaauw, B., C. Mammucari, L. Toniolo, L. Agatea, R. Abraham, M. Sandri, C. Reggiani, and S. Schiaffino. 2008. Akt activation prevents the force drop induced by eccentric contractions in dystrophin-deficient skeletal muscle. *Hum. Mol. Genet.* 17:3686–3696. http://dx.doi.org/10.1093/hmg/ddn264

Blaauw, B., M. Canato, L. Agatea, L. Toniolo, C. Mammucari, E. Masiero, R. Abraham, M. Sandri, S. Schiaffino, and C. Reggiani. 2009. Inducible activation of Akt increases skeletal muscle mass and force without satellite cell activation. *FASEB J.* 23:3896–3905. http://dx.doi.org/10.1096/fj.09-131870

Bodine, S.C., T.N. Stitt, M. Gonzalez, W.O. Kline, G.L. Stover, R. Bauerlein, E. Zlotchenko, A. Scrimgeour, J.C. Lawrence, D.J. Glass, and G.D. Yancopoulos. 2001. Akt/mTOR pathway is a crucial regulator of skeletal muscle hypertrophy and can prevent muscle atrophy in vivo. *Nat. Cell Biol.* 3:1014–1019. http://dx.doi.org/10.1038/ncb1101-1014

Burkin, D.J., and S.J. Kaufman. 1999. The alpha7beta1 integrin in muscle development and disease. *Cell Tissue Res.* 296:183–190. http://dx.doi.org/10.1007/s004410051279

Burkin, D.J., G.Q. Wallace, K.J. Nicol, D.J. Kaufman, and S.J. Kaufman. 2001. Enhanced expression of the α7β1 integrin reduces muscular dystrophy and restores viability in dystrophic mice. *J. Cell Biol.* 152:1207–1218. http://dx.doi.org/10.1083/jcb.152.6.1207

Burkin, D.J., G.Q. Wallace, D.J. Milner, E.J. Chaney, J.A. Mulligan, and S.J. Kaufman. 2005. Transgenic expression of alpha7beta1 integrin maintains muscle integrity, increases regenerative capacity, promotes hypertrophy, and reduces cardiomyopathy in dystrophic mice. *Am. J. Pathol.* 166:253–263. http://dx.doi.org/10.1016/S0002-9440(10)62249-3

Campbell, K.P., and S.D. Kahl. 1989. Association of dystrophin and an integral membrane glycoprotein. *Nature*. 338:259–262. http://dx.doi.org/10.1038/338259a0

Charrin, S., F. le Naour, O. Silvie, P.E. Milhiet, C. Boucheix, and E. Rubinstein. 2009. Lateral organization of membrane proteins: tetraspanins spin their web. *Biochem. J.* 420:133–154. http://dx.doi.org/10.1042/BJ20082422

Crosbie, R.H., J. Heighway, D.P. Venzke, J.C. Lee, and K.P. Campbell. 1997a. Sarcospan, the 25-kDa transmembrane component of the dystrophin-glycoprotein complex. *J. Biol. Chem.* 272:31221–31224. http://dx.doi.org/10.1074/jbc.272.50.31221

Crosbie, R.H., J. Heighway, D.P. Venzke, J.C. Lee, and K.P. Campbell. 1997b. Sarcospan, the 25-kDa transmembrane component of the dystrophin-glycoprotein complex. *J. Biol. Chem.* 272:31221–31224. http://dx.doi.org/10.1074/jbc.272.50.31221

Crosbie, R.H., C.S. Lebakken, K.H. Holt, D.P. Venzke, V. Straub, J.C. Lee, R.M. Grady, J.S. Chamberlain, J.R. Sanes, and K.P. Campbell. 1999a. Membrane targeting and stabilization of sarcospan is mediated by the sarcoglycan subcomplex. *J. Cell Biol.* 145:153–165. http://dx.doi.org/10.1083/jcb.145.1.153

Crosbie, R.H., C.S. Lebakken, K.H. Holt, D.P. Venzke, V. Straub, J.C. Lee, R.M. Grady, J.S. Chamberlain, J.R. Sanes, and K.P. Campbell. 1999b. Membrane targeting and stabilization of sarcospan is mediated by the sarcoglycan subcomplex. *J. Cell Biol.* 145:153–165. http://dx.doi.org/10.1083/jcb.145.1.153

Crosbie, R.H., L.E. Lim, S.A. Moore, M. Hirano, A.P. Hays, S.W. Maybaum, H. Collin, S.A. Dovico, C.A. Stolle, M. Fardeau, et al. 2000. Molecular and genetic characterization of sarcospan: insights into sarcoglycan-sarcospan interactions. *Hum. Mol. Genet.* 9:2019–2027. http://dx.doi.org/10.1093/hmg/9.13.2019

Deconinck, A.E., J.A. Rafael, J.A. Skinner, S.C. Brown, A.C. Potter, L. Metzinger, D.J. Watt, J.G. Dickson, J.M. Tinsley, and K.E. Davies. 1997a. Utrophin-dystrophin-deficient mice as a model for Duchenne muscular dystrophy. *Cell*. 90:717–727. http://dx.doi.org/10.1016/S0092-8674(00)80532-2

Deconinck, N., J. Tinsley, F. De Backer, R. Fisher, D. Kahn, S. Phelps, K. Davies, and J.M. Gillis. 1997b. Expression of truncated utrophin leads to major functional improvements in dystrophin-deficient muscles of mice. *Nat. Med.* 3:1216–1221. http://dx.doi.org/10.1038/nm1197-1216

Deol, J.R., G. Danialou, N. Larochelle, M. Bourget, J.S. Moon, A.B. Liu, R. Gilbert, B.J. Petrof, J. Nalbantoglu, and G. Karpati. 2007. Successful compensation for dystrophin deficiency by a helper-dependent adenovirus expressing full-length utrophin. *Mol. Ther.* 15:1767–1774. http://dx.doi.org/10.1038/sj.mt.6300260

Durko, M., C. Allen, J. Nalbantoglu, and G. Karpati. 2010. CT-GalNAc transferase overexpression in adult mice is associated with extrasynaptic utrophin in skeletal muscle fibres. *J. Muscle Res. Cell Motil.* 31:181–193. http://dx.doi.org/10.1007/s10974-010-9222-9

Ervasti, J.M. 2007. Dystrophin, its interactions with other proteins, and implications for muscular dystrophy. *Biochim. Biophys. Acta*. 1772:108–117.

Ervasti, J.M., and K.P. Campbell. 1991. Membrane organization of the dystrophin-glycoprotein complex. *Cell*. 66:1121–1131. http://dx.doi.org/10.1016/0092-8674(91)90035-W

Ervasti, J.M., and K.P. Campbell. 1993. A role for the dystrophin-glycoprotein complex as a transmembrane linker between laminin and actin. *J. Cell Biol.* 122:809–823. http://dx.doi.org/10.1083/jcb.122.4.809

Ervasti, J.M., K. Ohlendieck, S.D. Kahl, M.G. Gaver, and K.P. Campbell. 1990. Deficiency of a glycoprotein component of the dystrophin complex in dystrophic muscle. *Nature*. 345:315–319. http://dx.doi.org/10.1038/345315a0

Ervasti, J.M., S.D. Kahl, and K.P. Campbell. 1991. Purification of dystrophin from skeletal muscle. *J. Biol. Chem.* 266:9161–9165.

Fisher, R., J.M. Tinsley, S.R. Phelps, S.E. Squire, E.R. Townsend, J.E. Martin, and K.E. Davies. 2001. Non-toxic ubiquitous over-expression of utrophin in the mdx mouse. *Neuromuscul. Disord.* 11:713–721. http://dx.doi.org/10.1016/S0960-8966(01)00220-6

Galvagni, F., M. Cantini, and S. Oliviero. 2002. The utrophin gene is transcriptionally up-regulated in regenerating muscle. *J. Biol. Chem.* 277:19106–19113. http://dx.doi.org/10.1074/jbc.M109642200

García-Alvarez, B., J.M. de Pereda, D.A. Calderwood, T.S. Ulmer, D. Critchley, I.D. Campbell, M.H. Ginsberg, and R.C. Liddington. 2003. Structural determinants of integrin recognition by talin. *Mol. Cell*. 11:49–58. http://dx.doi.org/10.1016/S1097-2765(02)00823-7

Gilbert, R., J. Nalbantoglu, B.J. Petrof, S. Ebihara, G.H. Guibinga, J.M. Tinsley, A. Kamen, B. Massie, K.E. Davies, and G. Karpati. 1999. Adenovirus-mediated utrophin gene transfer mitigates the dystrophic phenotype of *mdx* mouse muscles. *Hum. Gene Ther.* 10:1299–1310. http://dx.doi.org/10.1089/10430349950017987

Grady, R.M., J.P. Merlie, and J.R. Sanes. 1997a. Subtle neuromuscular defects in utrophin-deficient mice. *J. Cell Biol.* 136:871–882. http://dx.doi.org/10.1083/jcb.136.4.871

Grady, R.M., H. Teng, M.C. Nichol, J.C. Cunningham, R.S. Wilkinson, and J.R. Sanes. 1997b. Skeletal and cardiac myopathies in mice lacking utrophin and dystrophin: a model for Duchenne muscular dystrophy. *Cell*. 90:729–738. http://dx.doi.org/10.1016/S0092-8674(00)80533-4

Grady, R.M., H. Zhou, J.M. Cunningham, M.D. Henry, K.P. Campbell, and J.R. Sanes. 2000. Maturation and maintenance of the neuromuscular synapse: genetic evidence for roles of the dystrophin—glycoprotein complex. *Neuron*. 25:279–293. http://dx.doi.org/10.1016/S0896-6273(00)80894-6

Gramolini, A.O., and B.J. Jasmin. 1999. Expression of the utrophin gene during myogenic differentiation. *Nucleic Acids Res.* 27:3603–3609. http://dx.doi.org/10.1093/nar/27.17.3603

Grewal, P.K., P.J. Holzfeind, R.E. Bittner, and J.E. Hewitt. 2001. Mutant glycosyltransferase and altered glycosylation of alpha-dystroglycan in the myodystrophy mouse. *Nat. Genet.* 28:151–154. http://dx.doi.org/10.1038/88865

Helliwell, T.R., N.T. Man, G.E. Morris, and K.E. Davies. 1992. The dystrophin-related protein, utrophin, is expressed on the sarcolemma of regenerating human skeletal muscle fibres in dystrophies and inflammatory myopathies. *Neuromuscul. Disord.* 2:177–184. http://dx.doi.org/10.1016/0960-8966(92)90004-P

Hijikata, T., T. Murakami, H. Ishikawa, and H. Yorifuji. 2003. Plectin tethers desmin intermediate filaments onto subsarcolemmal dense plaques containing dystrophin and vinculin. *Histochem. Cell Biol.* 119:109–123.

Hoffman, E.P., R.H. Brown Jr., and L.M. Kunkel. 1987. Dystrophin: the protein product of the Duchenne muscular dystrophy locus. *Cell*. 51:919–928. http://dx.doi.org/10.1016/0092-8674(87)90579-4

Holt, K.H., L.E. Lim, V. Straub, D.P. Venzke, F. Duclos, R.D. Anderson, B.L. Davidson, and K.P. Campbell. 1998. Functional rescue of the sarcoglycan complex in the BIO 14.6 hamster using delta-sarcoglycan gene transfer. *Mol. Cell*. 1:841–848. http://dx.doi.org/10.1016/S1097-2765(00)80083-0

Holzfeind, P.J., P.K. Grewal, H.A. Reitsamer, J. Kechvar, H. Lassmann, H. Hoeger, J.E. Hewitt, and R.E. Bittner. 2002. Skeletal, cardiac and tongue muscle pathology, defective retinal transmission, and neuronal migration defects in the Large(myd) mouse defines a natural model for glycosylation-deficient muscle - eye - brain disorders. *Hum. Mol. Genet.* 11:2673–2687. http://dx.doi.org/10.1093/hmg/11.21.2673

Hoyte, K., C. Kang, and P.T. Martin. 2002. Definition of pre- and postsynaptic forms of the CT carbohydrate antigen at the neuromuscular junction: ubiquitous expression of the CT antigens and the CT GalNAc transferase in mouse tissues. *Brain Res. Mol. Brain Res.* 109:146–160. http://dx.doi.org/10.1016/S0169-328X(02)00551-X

Ibraghimov-Beskrovnaya, O., J.M. Ervasti, C.J. Leveille, C.A. Slaughter, S.W. Sernett, and K.P. Campbell. 1992. Primary structure of dystrophin-associated glycoproteins linking dystrophin to the extracellular matrix. *Nature*. 355:696–702. http://dx.doi.org/10.1038/355696a0

Ibraghimov-Beskrovnaya, O., A. Milatovich, T. Ozcelik, B. Yang, K. Koepnick, U. Francke, and K.P. Campbell. 1993. Human dystroglycan: skeletal muscle cDNA, genomic structure, origin of tissue specific isoforms and chromosomal localization. *Hum. Mol. Genet.* 2:1651–1657. http://dx.doi.org/10.1093/hmg/2.10.1651

Izumiya, Y., T. Hopkins, C. Morris, K. Sato, L. Zeng, J. Viereck, J.A. Hamilton, N. Ouchi, N.K. LeBrasseur, and K. Walsh. 2008. Fast/Glycolytic muscle fiber growth reduces fat mass and improves metabolic parameters in obese mice. *Cell Metab.* 7:159–172. http://dx.doi.org/10.1016/j.cmet.2007.11.003

Jasmin, B.J., H. Alameddine, J.A. Lunde, F. Stetzkowski-Marden, H. Collin, J.M. Tinsley, K.E. Davies, F.M. Tomé, D.J. Parry, and J. Cartaud. 1995. Expression of utrophin and its mRNA in denervated mdx mouse muscle. *FEBS Lett.* 374:393–398. http://dx.doi.org/10.1016/0014-5793(95)01131-W

Kanagawa, M., F. Saito, S. Kunz, T. Yoshida-Moriguchi, R. Barresi, Y.M. Kobayashi, J. Muschler, J.P. Dumanski, D.E. Michele, M.B. Oldstone, and K.P. Campbell. 2004. Molecular recognition by LARGE is essential for expression of functional dystroglycan. *Cell*. 117:953–964. http://dx.doi.org/10.1016/j.cell.2004.06.003

Khurana, T.S., S.C. Watkins, P. Chafey, J. Chelly, F.M. Tomé, M. Fardeau, J.C. Kaplan, and L.M. Kunkel. 1991. Immunolocalization and developmental expression of dystrophin related protein in skeletal muscle. *Neuromuscul. Disord.* 1:185–194. http://dx.doi.org/10.1016/0960-8966(91)90023-L

Kim, M.H., D.I. Kay, R.T. Rudra, B.M. Chen, N. Hsu, Y. Izumiya, L. Martinez, M.J. Spencer, K. Walsh, A.D. Grinnell, and R.H. Crosbie. 2011. Myogenic Akt signaling attenuates muscular degeneration, promotes myofiber regeneration and improves muscle function in dystrophin-deficient mdx mice. *Hum. Mol. Genet.* 20:1324–1338. http://dx.doi.org/10.1093/hmg/ddr015

Lebakken, C.S., D.P. Venzke, R.F. Hrstka, C.M. Consolino, J.A. Faulkner, R.A. Williamson, and K.P. Campbell. 2000. Sarcospan-deficient mice maintain normal muscle function. *Mol. Cell. Biol.* 20:1669–1677. http://dx.doi.org/10.1128/MCB.20.5.1669-1677.2000

Litjens, S.H., K. Wilhelmsen, J.M. de Pereda, A. Perrakis, and A. Sonnenberg. 2005. Modeling and experimental validation of the binary complex of the plectin actin-binding domain and the first pair of fibronectin type III (FNIII) domains of the beta4 integrin. *J. Biol. Chem.* 280:22270–22277. http://dx.doi.org/10.1074/jbc.M411818200

Liu, J., D.J. Milner, M.D. Boppart, R.S. Ross, and S.J. Kaufman. 2012. β1D chain increases α7β1 integrin and laminin and protects against sarcolemmal damage in mdx mice. *Hum. Mol. Genet.* 21:1592–1603. http://dx.doi.org/10.1093/hmg/ddr596

Liu, L., B. He, W.M. Liu, D. Zhou, J.V. Cox, and X.A. Zhang. 2007. Tetraspanin CD151 promotes cell migration by regulating integrin trafficking. *J. Biol. Chem.* 282:31631–31642. http://dx.doi.org/10.1074/jbc.M701165200

Love, D.R., D.F. Hill, G. Dickson, N.K. Spurr, B.C. Byth, R.F. Marsden, F.S. Walsh, Y.H. Edwards, and K.E. Davies. 1989. An autosomal transcript in skeletal muscle with homology to dystrophin. *Nature*. 339:55–58. http://dx.doi.org/10.1038/339055a0

Martin, P.T. 2003. Glycobiology of the neuromuscular junction. *J. Neurocytol.* 32:915–929. http://dx.doi.org/10.1023/B:NEUR.0000020632.41508.83

Martin, P.T., and J.R. Sanes. 1995. Role for a synapse-specific carbohydrate in agrin-induced clustering of acetylcholine receptors. *Neuron*. 14:743–754. http://dx.doi.org/10.1016/0896-6273(95)90218-X

Martin, P.T., S.J. Kaufman, R.H. Kramer, and J.R. Sanes. 1996. Synaptic integrins in developing, adult, and mutant muscle: selective association of alpha1, alpha7A, and alpha7B integrins with the neuromuscular junction. *Dev. Biol.* 174:125–139. http://dx.doi.org/10.1006/dbio.1996.0057

Matsumura, K., J.M. Ervasti, K. Ohlendieck, S.D. Kahl, and K.P. Campbell. 1992. Association of dystrophin-related protein with dystrophin-associated proteins in mdx mouse muscle. *Nature*. 360:588–591. http://dx.doi.org/10.1038/360588a0

Michele, D.E., R. Barresi, M. Kanagawa, F. Saito, R.D. Cohn, J.S. Satz, J. Dollar, I. Nishino, R.I. Kelley, H. Somer, et al. 2002. Post-translational disruption of dystroglycan-ligand interactions in congenital muscular dystrophies. *Nature*. 418:417–422. http://dx.doi.org/10.1038/nature00837

Miller, G., E.L. Wang, K.L. Nassar, A.K. Peter, and R.H. Crosbie. 2007. Structural and functional analysis of the sarcoglycan-sarcospan subcomplex. *Exp. Cell Res.* 313:639–651. http://dx.doi.org/10.1016/j.yexcr.2006.11.021

Nguyen, H.H., V. Jayasinha, B. Xia, K. Hoyte, and P.T. Martin. 2002. Overexpression of the cytotoxic T cell GalNAc transferase in skeletal muscle inhibits muscular dystrophy in mdx mice. *Proc. Natl. Acad. Sci. USA*. 99:5616–5621. http://dx.doi.org/10.1073/pnas.082613599

Nguyen, T.M., J.M. Ellis, D.R. Love, K.E. Davies, K.C. Gatter, G. Dickson, and G.E. Morris. 1991. Localization of the DMDL gene-encoded dystrophin-related protein using a panel of nineteen monoclonal antibodies: presence at neuromuscular junctions, in the sarcolemma of dystrophic skeletal muscle, in vascular and other smooth muscles, and in proliferating brain cell lines. *J. Cell Biol.* 115:1695–1700. http://dx.doi.org/10.1083/jcb.115.6.1695

Odom, G.L., P. Gregorevic, J.M. Allen, E. Finn, and J.S. Chamberlain. 2008. Microutrophin delivery through rAAV6 increases lifespan and improves muscle function in dystrophic dystrophin/utrophin-deficient mice. *Mol. Ther.* 16:1539–1545. http://dx.doi.org/10.1038/mt.2008.149

Pallafacchina, G., E. Calabria, A.L. Serrano, J.M. Kalhovde, and S. Schiaffino. 2002. A protein kinase B-dependent and rapamycin-sensitive pathway controls skeletal muscle growth but not fiber type specification. *Proc. Natl. Acad. Sci. USA*. 99:9213–9218. http://dx.doi.org/10.1073/pnas.142166599

Percival, J.M., P. Gregorevic, G.L. Odom, G.B. Banks, J.S. Chamberlain, and S.C. Froehner. 2007. rAAV6-microdystrophin rescues aberrant Golgi complex organization in *mdx* skeletal muscles. *Traffic*. 8:1424–1439. http://dx.doi.org/10.1111/j.1600-0854.2007.00622.x

Peter, A.K., and R.H. Crosbie. 2006. Hypertrophic response of Duchenne and limb-girdle muscular dystrophies is associated with activation of Akt pathway. *Exp. Cell Res.* 312:2580–2591. http://dx.doi.org/10.1016/j.yexcr.2006.04.024

Peter, A.K., G. Miller, and R.H. Crosbie. 2007. Disrupted mechanical stability of the dystrophin-glycoprotein complex causes severe muscular dystrophy in sarcospan transgenic mice. *J. Cell Sci.* 120:996–1008. http://dx.doi.org/10.1242/jcs.03360

Peter, A.K., J.L. Marshall, and R.H. Crosbie. 2008. Sarcospan reduces dystrophic pathology: stabilization of the utrophin–glycoprotein complex. *J. Cell Biol.* 183:419–427. http://dx.doi.org/10.1083/jcb.200808027

Peter, A.K., C.Y. Ko, M.H. Kim, N. Hsu, N. Ouchi, S. Rhie, Y. Izumiya, L. Zeng, K. Walsh, and R.H. Crosbie. 2009. Myogenic Akt signaling upregulates the utrophin-glycoprotein complex and promotes sarcolemma stability in muscular dystrophy. *Hum. Mol. Genet.* 18:318–327. http://dx.doi.org/10.1093/hmg/ddn358

Petrof, B.J., J.B. Shrager, H.H. Stedman, A.M. Kelly, and H.L. Sweeney. 1993. Dystrophin protects the sarcolemma from stresses developed during muscle contraction. *Proc. Natl. Acad. Sci. USA*. 90:3710–3714. http://dx.doi.org/10.1073/pnas.90.8.3710

Rafael, J.A., J.M. Tinsley, A.C. Potter, A.E. Deconinck, and K.E. Davies. 1998. Skeletal muscle-specific expression of a utrophin transgene rescues utrophin-dystrophin deficient mice. *Nat. Genet.* 19:79–82. http://dx.doi.org/10.1038/ng0598-79

Ramaswamy, K.S., M.L. Palmer, J.H. van der Meulen, A. Renoux, T.Y. Kostrominova, D.E. Michele, and J.A. Faulkner. 2011. Lateral transmission of force is impaired in skeletal muscles of dystrophic mice and very old rats. *J. Physiol.* 589:1195–1208. http://dx.doi.org/10.1113/jphysiol.2010.201921

Rezniczek, G.A., P. Konieczny, B. Nikolic, S. Reipert, D. Schneller, C. Abrahamsberg, K.E. Davies, S.J. Winder, and G. Wiche. 2007. Plectin 1f scaffolding at the sarcolemma of dystrophic (*mdx*) muscle fibers through multiple interactions with β-dystroglycan. *J. Cell Biol.* 176:965–977. http://dx.doi.org/10.1083/jcb.200604179

Rommel, C., S.C. Bodine, B.A. Clarke, R. Rossman, L. Nunez, T.N. Stitt, G.D. Yancopoulos, and D.J. Glass. 2001. Mediation of IGF-1-induced skeletal myotube hypertrophy by PI(3)K/Akt/mTOR and PI(3)K/Akt/GSK3 pathways. *Nat. Cell Biol.* 3:1009–1013. http://dx.doi.org/10.1038/ncb1101-1009

Rooney, J.E., J.V. Welser, M.A. Dechert, N.L. Flintoff-Dye, S.J. Kaufman, and D.J. Burkin. 2006. Severe muscular dystrophy in mice that lack dystrophin and alpha7 integrin. *J. Cell Sci.* 119:2185–2195. http://dx.doi.org/10.1242/jcs.02952

Smith, P.L., and J.B. Lowe. 1994. Molecular cloning of a murine N-acetylgalactosamine transferase cDNA that determines expression of the T lymphocyte-specific CT oligosaccharide differentiation antigen. *J. Biol. Chem.* 269:15162–15171.

Sonnemann, K.J., H. Heun-Johnson, A.J. Turner, K.A. Baltgalvis, D.A. Lowe, and J.M. Ervasti. 2009. Functional substitution by TAT-utrophin in dystrophin-deficient mice. *PLoS Med.* 6:e1000083. http://dx.doi.org/10.1371/journal.pmed.1000083

Squire, S., J.M. Raymackers, C. Vandebrouck, A. Potter, J. Tinsley, R. Fisher, J.M. Gillis, and K.E. Davies. 2002. Prevention of pathology in mdx mice by expression of utrophin: analysis using an inducible transgenic expression system. *Hum. Mol. Genet.* 11:3333–3344. http://dx.doi.org/10.1093/hmg/11.26.3333

Straub, V., J.A. Rafael, J.S. Chamberlain, and K.P. Campbell. 1997. Animal models for muscular dystrophy show different patterns of sarcolemmal disruption. *J. Cell Biol.* 139:375–385. http://dx.doi.org/10.1083/jcb.139.2.375

Takahashi, A., Y. Kureishi, J. Yang, Z. Luo, K. Guo, D. Mukhopadhyay, Y. Ivashchenko, D. Branellec, and K. Walsh. 2002. Myogenic Akt signaling regulates blood vessel recruitment during myofiber growth. *Mol. Cell. Biol.* 22:4803–4814. http://dx.doi.org/10.1128/MCB.22.13.4803-4814.2002

Tinsley, J.M., A.C. Potter, S.R. Phelps, R. Fisher, J.I. Trickett, and K.E. Davies. 1996. Amelioration of the dystrophic phenotype of *mdx* mice using a truncated utrophin transgene. *Nature*. 384:349–353. http://dx.doi.org/10.1038/384349a0

Tinsley, J., N. Deconinck, R. Fisher, D. Kahn, S. Phelps, J.M. Gillis, and K. Davies. 1998a. Expression of full-length utrophin prevents muscular dystrophy in *mdx* mice. *Nat. Med.* 4:1441–1444. http://dx.doi.org/10.1038/4033

Tinsley, J., N. Deconinck, R. Fisher, D. Kahn, S. Phelps, J.M. Gillis, and K. Davies. 1998b. Expression of full-length utrophin prevents muscular dystrophy in *mdx* mice. *Nat. Med.* 4:1441–1444. http://dx.doi.org/10.1038/4033

Vivanco, I., and C.L. Sawyers. 2002. The phosphatidylinositol 3-kinase AKT pathway in human cancer. *Nat. Rev. Cancer*. 2:489–501. http://dx.doi.org/10.1038/nrc839

Xia, B., K. Hoyte, A. Kammesheidt, T. Deerinck, M. Ellisman, and P.T. Martin. 2002. Overexpression of the CT GalNAc transferase in skeletal muscle alters myofiber growth, neuromuscular structure, and laminin expression. *Dev. Biol.* 242:58–73. http://dx.doi.org/10.1006/dbio.2001.0530

Xu, R., M. Camboni, and P.T. Martin. 2007a. Postnatal overexpression of the CT GalNAc transferase inhibits muscular dystrophy in mdx mice without altering muscle growth or neuromuscular development: evidence for a utrophin-independent mechanism. *Neuromuscul. Disord.* 17:209–220. http://dx.doi.org/10.1016/j.nmd.2006.12.004

Xu, R., K. Chandrasekharan, J.H. Yoon, M. Camboni, and P.T. Martin. 2007b. Overexpression of the cytotoxic T cell (CT) carbohydrate inhibits muscular dystrophy in the dyW mouse model of congenital muscular dystrophy 1A. *Am. J. Pathol.* 171:181–199. http://dx.doi.org/10.2353/ajpath.2007.060927

Yoshida, M., and E. Ozawa. 1990. Glycoprotein complex anchoring dystrophin to sarcolemma. *J. Biochem.* 108:748–752.

Yoshida-Moriguchi, T., L. Yu, S.H. Stalnaker, S. Davis, S. Kunz, M. Madson, M.B. Oldstone, H. Schachter, L. Wells, and K.P. Campbell. 2010. O-mannosyl phosphorylation of alpha-dystroglycan is required for laminin binding. *Science*. 327:88–92. http://dx.doi.org/10.1126/science.1180512

Zhao, J., K. Yoshioka, M. Miyatake, and T. Miike. 1992. Dystrophin and a dystrophin-related protein in intrafusal muscle fibers, and neuromuscular and myotendinous junctions. *Acta Neuropathol.* 84:141–146. http://dx.doi.org/10.1007/BF00311386